Chapter 5

SEDIMENTARY FACIES: PALAEOSOLS AND CALCRETES

5. SEDIMENTARY FACIES: PALAEOSOLS AND CALCRETES

The Quaternary stratigraphic record of Mainland Gujarat is replete with ancient soils (palaeosols) and secondary carbonate accumulations. These form generally due to the interaction of water and organic matter in areas of non-deposition in the uppermost layers of the earth's crust. In the present study the definitions for ancient soils provided by Mack et al., (1993) are followed. These are different from soil orders as defined in existing soil classification guidebooks (Soil Survey Staff, 1975). Mack et al., (1993) have justified why present day Soil Taxonomy is inapplicable directly to palaeosols. They argue:

> *'The primary problem is that many features critical to classification of modern soils, such as bulk density, cation exchange capacity, moisture content, and base status, do not survive into the rock record... Although it may be possible to estimate some of these properties, a consistent, quantitative determination is not possible. Even those pedogenic features that persist in paleosols are commonly modified from their original state by chemical diagenesis and compaction.*
>
> *...A second problem is that many soil classifications, Soil Taxonomy in particular..., depend in part upon knowledge of climatic conditions to properly classify a soil... It is unlikely that any paleoclimatic indicator or paleoclimatic model can provide such specific information for an ancient stratigraphic unit or time interval.'*

Based on these rationale they proposed a classification based on macroscopic features that were relatively resistant to diagenetic alteration and that which were not

severely affected by physical compaction. The flow chart of palaeosol orders is reproduced here (Fig. 5.1) along with the subordinate modifiers of palaeosols that will be followed (Table 5.1).

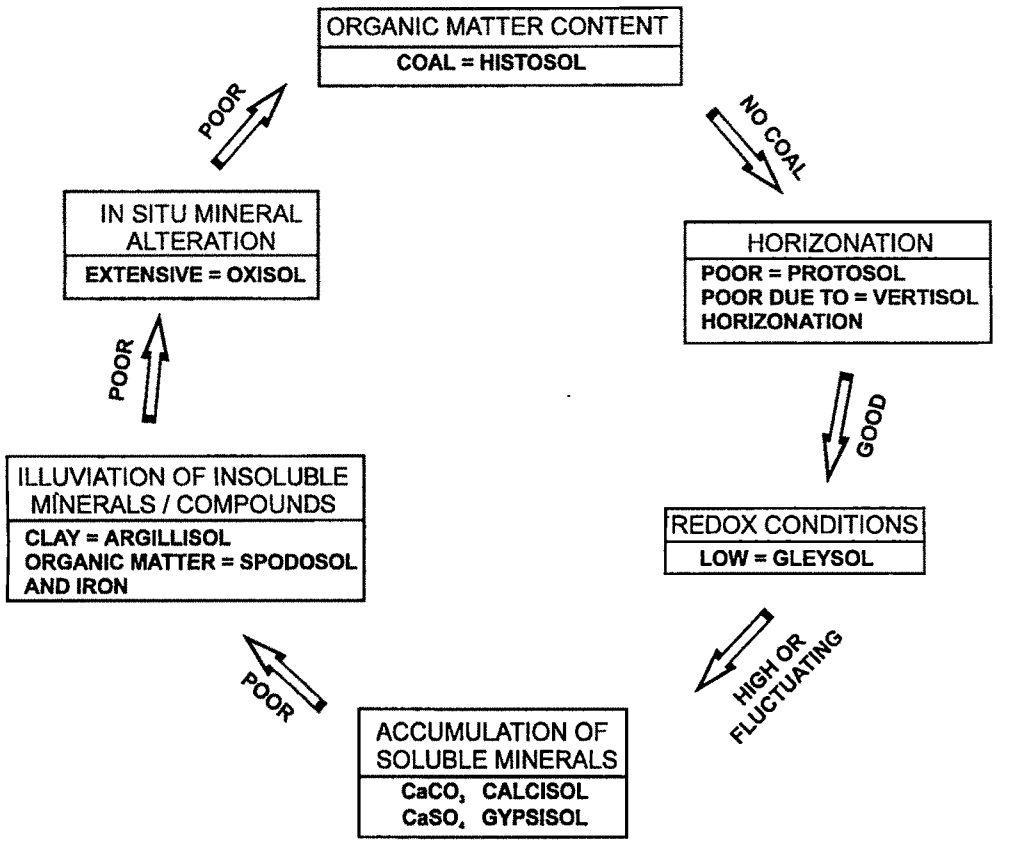

Figure 5.1: Classification of palaeosols (Mack et al., 1993)

It is a common practice amongst geologists to interpret soils in terms of landscape stability and no sedimentation. This leads to incorrect interpretations that periods in the stratigraphic record represented by palaeosols are times when deposition or aggradation was absent ubiquitously. While this may hold some truth in aeolian environments it is not correct for alluvial settings. With alluvial depositional systems, at the same stratigraphic level clastics and non-clastics (palaeoalterites) coexist and grade into each other (Bown & Kraus, 1987).

Modifier	Description
Albic	Presence of eluvial (E) horizon
Allophanic	Presence of allophane or other Si and Al compounds
Argillic	Presence of illuvial clay
Calcic	Presence of pedogenic carbonate
Cabonaceous	Presence of dark organic matter but not coal
Concretionary	Presence of glaebules with a concentric fabric
Dystric	Low base status as indicated by the paucity of chemically unstable grains such as feldspars and volcanic rock fragments
Eutric	High base status as indicated by the abundance of chemically unstable grains such as feldspars and volcanic rock fragments
Ferric	Presence of iron oxides
Fragic	Subsurface horizon that was hard at the time of soil formation (for example, root traces and burrows terminate or are diverted at this horizon
Gleyed	Evidence of periodic water logging, such as drab hues; mottles of drab colours and yellow, red, or brown; or presence of pedogenic pyrite or siderite
Gypsic	Presence of vadose gypsum or anhydrite
Nodular	Presence of glaebules with an undifferentiated internal fabric
Ochric	Presence of light-coloured A horizon
Salic	Presence of pedogenic salts more soluble than gypsum
Silicic	Presence of pedogenic silica
Vertic	Presence of decimetre-scale desiccation cracks, wedge-shaped peds, hummock and swale structures, slickensides, or clastic dikes
Vitric	Presence of relict or actual glass shards or pumice

Table 5.1: Modifiers of palaeosols and their definitions (Mack et al., 1993)

Soils evolve over prolonged periods of time which is usually in the order of 10^3-10^6 years (Jenny, 1941). Hence, features such as clay accumulations, may result under reduced rates of weathering spanning a long period of time or at rapid rates of weathering over a short period of time under different climatic conditions. These complexities were

best exemplified by Jenny (1941) who demonstrated that the formation of a soil is governed by several factors operating in tandem with each other. This is given as:

$$s = f(cl, o, r, p, t)$$

wherein, 's' represents soil, 'cl' climate, 'o' organisms, 'r' topography (relief), 'p' parent material, and 't' time.

Calcrete nodules are described following essentially sedimentological nomenclature. However some terms that are more apt descriptors have been used from pedological literature. Carbonate nodules are considered different from carbonate concretions; the usage of the latter necessitating concentric growth. Carbonate nodules (calcretes) are classified as orthic, disorthic and allothic (Wieder & Yaalon, 1974). *Orthic* nodules are those in which siliciclastic (skeletal) grains contained in the nodule are the same as those in the host sediment, and in which the nodule boundary is diffuse. *Disorthic* nodules are similar to orthic nodules except for the sharp nodule boundaries indicative of pedoturbation (soil movement due to organic activity and moisture-controlled clay volume changes). *Allothic* nodules show differences between skeletal grain and host sediment mineralogical composition and are principally transported nodules.

The first part of this chapter introduces the principal soil types and their genesis. In the later part an attempt is made to describe various forms of calcretes of groundwater, pedogenic and rhizogenic origin, their formative pathways and sinks. An assessment of existing definitions of calcrete forms the concluding part wherein a modified definition of calcrete is proposed.

5.1 Vertisols

At the base of most sites dark coloured clays are commonly observed (Plate 5.1). The clays are brown to grayish brown in colour (7.5 YR 5/4). The clay-rich horizons display

an incremental decrease in clay content manifested in a loss of sediment cohesion down the profile. An exception to the usual is seen at Mahudi wherein the clays form a homogenous massive bed. Clay beds are usually 1.5 to 1.7 m thick. A most striking character of these is the development of concave up curvi-planes (Plate 5.2). The planes occur in two sets that are oppositely oriented. The intersection of these causes the clays to be organized in wedge shaped parallelepipeds. The spacing between successive planes varies between 10-15 cm. Where two oppositely directed planes cut across each other at the top of the profile, teepee-like structures result. The wedges show smaller curvi-planar discontinuities but they are poorly defined.

Along the planes, usually polished surfaces showing sub-parallel striations are present. These striations are caused by preferential orientation of clay particles (Plate 5.3). The presence of coarser particles (small basalt and calcrete clasts) leads to the formation of ridges and grooves that are spaced in a parallel to sub-parallel fashion.

Downward tapering fissures are seen in some profiles (Plate 5.4). The fissures are impregnated by calcium carbonate or are infilled by the overlying sediment or the clays themselves. The fissures range in width from 1 cm to 4 cm and rarely extend downward in a straight manner. More often they are sinuous and obliquely directed.

Drab coloured (greenish grey) haloes are observed throughout the profile. The haloes consist of a white calcium carbonate rich core enveloped by greenish grey clays translating outwards gradually into the host grey clays.

Mineralogical analyses were carried out on bulk powdered samples using a Phillips X Ray diffractometer (PW 1729) with a CuKα source. A more systematic clay mineral study has already been carried out earlier (Malik et al., 1998; Sareen & Tandon, 1995) using oriented clay slide mounts on which the effect of glycolation and heating was observed to enable clay mineral identification. For the present study a more cursory analysis was done to

support or verify this data. These analyses reveal a overwhelming presence of montomorillonite-smectite which shows peaks at 15.2-15.7 Å and 4.97-4.98 Å. The presence of vermiculite was identified by the 14.2-14.4 Å peak although similar values are also obtained for chloritic minerals. Kaolinite peaks were observed at values of 7.15-7.16 Å and 3.57 Å while peaks at 9.85-9.99 Å expressed the presence of illite in the sample. Quartz was present throughout the sample (3.34 Å and 4.26 Å). Based on the relative intensities of the peak the general relative abundances may be put as:

Montmorillonite >>> Kaolinite > Illite > Quartz

The presence of intense fracturing resulting in well-defined subangular aggregates reflects pedogenic activity. These aggregates are similar to features in modern soils that have been described as peds (Retallack, 1990). Peds form through repeated expansion and shrinkage of clays coupled with rooting activity of plants. Concave upward planes are interpreted as pseudo-anticlines. Such structures are the subsurface expression of surface microrelief known as gilgai (Wilding and Tessier, 1988; Coulombe et al., 1996). Further evidence of soil movement is seen in the linear striae (slickensides) along ped faces. The combined presence of wedge shaped or parallelepiped structural aggregates and slickensides is termed as 'vertic structure'.

Pseudo-anticlines and slickensides form in vertic soils when shear stresses exceed soil strength. Swelling pressures in such soils are about four times greater than vertical stresses. Slickensides consequently form when large swelling capacities in spatially constrained soils enable lateral movement. Theoretically the angle of shearing is equal to (45-O/2) wherein O is the angle of internal friction and as a rule is small for clay rich soils (Yaalon & Kalmar, 1978). Near the surface the downward component of resistance (overload) becomes negligible compared to the lateral component. Hence the soil mass moves vertically upwards. This interaction between shear stresses and overburden leads

to the formation of bowl (in the third dimension) (Wilding & Tessier, 1988). Slickensides form during the shearing when clays are smeared and oriented leading to the overall reduction in the pore size. Once established a given slickenside forms a surface of minimal resistance to shear during forthcoming wetting events and are thus maintained over long periods of time (Lynn & Williams, 1992).

Vertical fissures form in response to extreme drying events when the soil starts cracking. These cracks are subsequently infilled by detrital sediment or overlying collapsing soil matter or calcium carbonate precipitating from incoming solutions. Calcium carbonate in some fissures probably formed from carbonate rich waters that settled in these cracks as the channel avulsed on to the floodplain. The dominance of smectite clay and the presence of morphogenetic features such as vertical fissures, slickensides and pseudo-anticlines suggest that the soil belongs to the order Vertisol (Ahmad, 1983; Coulombe et al., 1996). Calcium carbonate nodules within these vertisols have sharply defined boundaries. This again suggests pedoturbation (Wieder and Yaalon, 1974). Cracked nodule surfaces reflect that soil shrinkage processes affected the nodules also. Strata-discordant tubes are interpreted as rhizoliths based on their bifurcation direction along with the progressive decrease in carbonate content outwards from the core (Klappa, 1980).

5.2 Red beds

Throughout both the basins a conspicuous red-bed horizon bisects the section at most sites (Plate 5.1). These red-beds are yellowish red to brick red in colour (5YR 5/6). They vary in thickness from about 1.5 m to as much as 4 m (at Dabka). The sediments at times have a wavy undulating upper surface which shows shallow mounds and depressions and has a sharp contact with the overlying light yellow coloured sediments of the Sh facies (Plate 5.5). Down profile the redness of the sediment progressively diminishes. This incremental

decrease is matched with loss in sediment cohesion (Plate 5.6). At the base of such profiles a zone of calcium carbonate nodules around 5 m thick is present.

Elsewhere (Oran, Aglod) within the red-beds sedimentary structures such as cross stratification are observed (Plate 5.7). In such cases the red beds have less clay content (judged by the stickiness of sediment in the field after applying a drop of water). Moreover the reddening is of a massive nature having relatively abrupt basal boundaries.

Where clay percentages are higher the beds are usually fine grained and may be classified as sandy loam. In these beds the samples are poor in fresh feldspar. On the other hand massive beds are rich in alkali feldspars (orthoclase), basaltic lithoclasts and calcrete lenses.

Clay mineralogy carried out on four bulk samples show abundance in montmorillonite (15.2-15.7 Å and 4.97-4.98 Å) followed by kaolinite (7.15-7.16 Å and 3.57 Å), illite (9.85-9.99 Å) and quartz (3.34 Å and 4.26 Å).

Montmorillonite>>Kaolinite>Illite>Quartz

Surprisingly no signatures of either haematite, goethite or gibbsite are seen in the diffractograms.

Red-coloured sediments have been reported from regions around the world and may be of both pedogenic as well as groundwater origin (Gardner & Pye, 1981; Pye, 1983). In the Mahi and Sabarmati basins a relatively clear distinction can be attempted using the following criteria. If red-beds were of pedogenic origin there would not have been abundant fresh feldspars. This provides a criterion to differentiate red-beds of detrital or groundwater origin. Additionally in the former case structures suggestive of mechanical transport are common. On the other hand in situ red beds seldom have large quanta of fresh feldspars. This, combined with clay accumulation, calcium carbonate nodules and a gradual decrease in the intensity of reddening down-profile characterizes pedogenic red beds. Red-bed

formation requires compulsive oxidizing conditions achieved by a free drainage conditions (no water logging). The red beds of pedogenic origin may be classified in the scheme of Mack et al., (1993) as ferric calcisols.

The brick red reddening is ascribed usually to the presence of fine particulate hematite. Lack of sufficient crystallinity may have been responsible presently for the absence of X-Ray signatures in the diffractograms (Pye, 1983).

The formation of hematite proceeds through dehydration of the primary weathering product of iron rich minerals (Schmalz, 1968). It may form by one of the following reaction paths:

$$2Fe(OH)_3 \leftrightarrow Fe_2O_3 + 3H_2O$$

$$2Fe(OH)_3 \leftrightarrow 2HFeO_2$$

$$2HFeO_2 + 2H_2O \leftrightarrow Fe_2O_3 + 3H_2O$$

$$2HFeO_2 \leftrightarrow Fe_2O_3 + H_2O$$

Schmalz (1968) raised the question whether or not hematite can form in the presence of liquid water replying to models put forth by (Walker, 1967). Using thermodynamic arguments he demonstrated that under standard conditions hematite cannot form stably in the presence of liquid water. The stability of either hematite and goethite is governed by the activity of water which does not form a parameter in mineral-stability fence diagrams. Consequently the formation of hematite would thus require very high temperatures or environments wherein the activity of water is considerably reduced. The activity of water may be also reduced through the presence of dissolved salts. Moreover once formed, the reversible reaction involving the hydration of hematite to form goethite is an extremely sluggish process.

Hence the formation of pedogenic hematite would thus require 1) enough moisture so as to enable chemical weathering of primary minerals and 2) low activity of water, that

would propel dehydration. Such ideal conditions are met with in tropical savannas where climatic seasonality provides a means of satisfying both the above requirements.

In a red-bed kind of landscape, pedogenically reddened sediments would tend to be eroded during rain bearing months. This would result in the reddening of waters through the entrainment of hematite as colloidal particles in the suspension load. Sediments deposited from such red coloured waters would contain evidences of transport and would be devoid of weathered minerals. Expected complications include the pedogenesis of floodplains which have received reddened sediments from the rivers. In such cases it would be very difficult to separate and recognize both processes.

5.3 Calcretes: macroscopic features

5.3.1 Pedogenic calcretes

Associated with vertisols and red-soil are observed calcareous nodules of varying sizes and shapes (Plates 5.1, 5.4, 5.8, 5.9, 5.10, 5.11). The nodules range in colour from pure white to light grey to light brown. The degree of whiteness reflects the amount of non-carbonate material in it. Nodule sizes range from sub-centimetre to as much as 12 cm in diameter. In a given soil profile sub-centimetre nodules are distributed throughout the profile whereas nodules >6 cm are less profusely developed.

The morphology of nodules varies from roughly conical to sub-spherical to irregular. Popcorn-like structures as well as nodule-coalescence are not observed. At Rayka, vertisols show a unique form of calcrete in which the core shows the presence of a nucleus. The relative size of the nucleus which is a clay aggregate (ped) varies in comparison to the whole nodule. In the most extreme of cases the nucleus forms the bulk of the nodule and the calcium carbonate cemented area envelopes it to forms a 2-5 mm thick protective shell. These nodules show a high degree of sphericity and more often

than not appear as balls. The nodules are disorthic (Wieder & Yaalon, 1974), meaning that they show a sharp boundary with the host sediment, in this case the soil matrix. Carbonates also form along vertical fissures extending from the top of the profile and tapering downwards.

Elsewhere where the degree of hydromorphism is more (e.g. Rayka, Mahudi) the calcretes are more massive and more carbonate rich (Plate 5.9, 5.11). These nodules are also disorthic. The nodules are pure white in colour and show sub-spherical to irregular morphologies. The distribution of the nodules is not at a particular depth but may be present at any depth in the profile. At the surface of some nodules, slickensides akin to those developed on clay peds are observed. This feature is most well developed at Mahudi (Sabarmati). The nodules are fine grained with sparitic veins cutting across randomly (Plate 5.11). The surface morphology is highly irregular excluding the parts where slickensides are developed. Cracks extending inwards from the surface are common in some. These cracks are usually filled with clay.

Calcretes associated with the red-soil are usually between 1-3 cm in diameter. These disorthic nodules are white in colour and are enriched with respect to calcium carbonate (Plate 5.10). The nodules are spheroidal in shape and have rather smooth surfaces. They usually form a zone 0.5 m thick which occurs at varying depths at different localities. At places it is observed that such zones (but less thick) are separated by a zone devoid of calcretes.

The intimate association of carbonate nodules with soil profiles suggests a pedogenic origin. This is supported by the disorthic nature of the nodules (Wieder & Yaalon, 1974). The nodules show evidences of shrinkage in the form of sparitic veins. The formation of the nodules took place by the downward leaching of calcium carbonate. This leaching may have taken place either along primary porosities or secondary

porosities. The role of inter-pedal planes in generating secondary porosity has largely been accepted (e.g. Wieder & Yaalon, 1974). The presence of slickensides on the calcrete nodule surface attests to this hypothesis. Moreover it appears that in vertisol calcretes the peds act as nuclei around which precipitation of calcium carbonate has been initiated. Such nodule types have not been reported. Whereas it is clear when examining thin-shell nodules that a nucleus is present, in the more thick-shelled nodules, the amount of calcium carbonate in the nodule may be over-estimated if assessed on the basis of surface morphology itself. Large nodule sizes have been documented from hydromorphic soils by Aslan & Kraus (1993). The massive nature of nodules in hydromorphic soils may be due to the very nature of water logging which retains water rich in calcium carbonate by impeding its drainage down the soil profile. Fissures also provide conduits along which calcium carbonate precipitates in the vertic calcretes. Calcium carbonate precipitated either by evaporation or by carbon dioxide degassing evaporation, or the common-ion effect or possibly all the three processes together (Wright & Tucker, 1991). Calcretes associated with vertisols have also been commonly recorded in older fluvial successions (Driese & Mora, 1993; Caudill et al., 1996).

5.3.2 Groundwater calcretes

Soft carbonate nodules showing diffused margins with the host sediment are the components of this variety. The host sediment usually comprises stratified silts and fine sands. The diffuse-margin nodules occur in layers which conform with the stratification of the sediment body. Such carbonate sheets are seen to follow stratal planes of channels and mimic the concave-up geometry of the channel-fill deposits. The nodules range in size from 1 to 3 cm in width to continuous sheets of carbonate (Plates 5.1, 5.12, 5.13). The calcrete sheets are usually 2-3 cm thick but at times also reaches upto 7 cm in

thickness and are contiguous over several decimetres. Where the sheets are thicker the carbonate segregation is limited and it appears more like highly calcified sediment. The colour of the nodules varies from buff to pure white, reflecting the increasing amount of calcium carbonate. Some of the carbonate sheets also show surface cracking. The nodules range in their external form from subspherical to knobby (popcorn-like) to highly irregular. In some cases where the nodules occur in layers stratification discordant nodules are also observed which connect the layers.

The presence of carbonate nodules and sheets along stratification planes indicates that the carbonates formed inorganically either from laterally migrating groundwaters travelling preferentially along such planes (Netterberg, 1969, 1974), or from ponded waters in channels (Arakel, 1986). The precipitation in the latter case was probably aided by the near-surface water flow along the river conduits. Calcium carbonate precipitated from these groundwaters either by evaporation or by carbon dioxide degassing (Spötl and Wright, 1992). As in the case of pedogenic calcretes, $CaCO_3$ precipitates through CO_2 degassing, evaporation, or the common-ion effect or possibly all the three processes together.

The occurrence of groundwater as bands suggests that each foreset bed or stratum acted as a local perched aquifer. Normal grading within these deposits probably led to the formation of clay rich tops of a stratum. Fine grained sediments tend to be preferentially cemented (Lang et al., 1990) which is apparently due to higher pore-fluid retention capacities (Gardner & McLaren, 1994).

In the Lake Napperby area, central Australia, calcretes form along trunk channels and reach a thickness of up to several decimetres (Arakel & McConchie, 1982; Arakel, 1986). Similarly in southern Africa river sands are usually impregnated with calcium carbonate (Netterberg, 1969). Groundwater calcretes are also being increasingly

recognised in older sediments (Pimentel et al., 1996; Tandon & Gibling, 1997). Tandon & Gibling (1997) reported bedding concordant carbonate cemented layers 20 cm thick and 3 m wide. Such layers have been confused with palustrine carbonates as is the case from the Permian strata of the Karoo Province (Smith, 1990). He described <5 cm thick sheets that crop out as continuous ledges. As in the present case the upper surfaces of these sheets are sharp and flat while the lower boundary is gradational. These calcretes are comparable with the groundwater calcretes from Mainland Gujarat.

5.3.3 Cauliflower calcretes

The need to form one more category came about because of the unique character of these calcretes. At Mahudi (Sabarmati), a 4-5 m thick clay horizon above vertisol-2 (Plates 5.1, 5.14, 5.15) is present which contains light brown calcareous nodules that on an average are 5-15 cm in diameter. The nodules are largely hemi-spheroidal in form but smaller nodules are spheroidal in shape. The nodules are replete with innumerable sinuous cracks that forms a mesh running over the surface of the nodule. The cracks are commonly upto 3 mm wide and form a negative topography and extend into the host clay also. The density of cracks is less and the intersection of these define polygons of carbonate rich clay. The nodules are present throughout the unit but show no discernible trend. The unit has been traced laterally for about 100-150 m, however the exact extent is unknown. Cut slabs of these nodules show that the sinuous inward tapering cracks are in-filled with either clay or clear sparite. Siliciclastic detritus is less in concentration, and micrite rich layers seen as whiter patches are common.

The profuse distribution of nodules through the unit suggests a system in which there was no dearth in the supply of Ca^{2+} ions. The unit is also rich in montmorillonitic clay indicating low energy conditions. Shrinkage of this clay led to the development of cracks that extended into the nodules also. Such shrinkage took place episodically as is

reflected in the multiple generations of sparitic veins. It has been difficult to find any description of both modern or ancient analogues which might be used for comparison. The nodules cannot be compared with septarian nodules since in the latter cracks radiate outwards from the centre of the nodule and taper towards the rim. The surface morphology mimics that of cauliflowers and hence is used as a classification term.

Using Walther's law one would expect the environment of formation to be away or adjacent to regions of vertisol formation (as it is underlain by one). Such areas are backswamps and are regions of negative relief forming depressions. These calcretes probably formed in one such depression that was ephemerally ponded and received clay episodically through overbank floods. Since no horizonation is seen in the clays it is surmised that the unit is a depositional one and hence the clays are derived or transported. Cauliflower calcretes thus represent a unique transition from true pedogenic calcretes to palustrine carbonates (Alonso Zarza et al., 1992) showing a larger role of shrinkage processes.

5.3.4 Rhizogenic calcretes

Rhizogenic calcretes or calcretes that form through physico-chemical processes in the root zone are less common in the stratigraphic record (Plates 5.1, 5.16, 5.17). When present they occur as straight to sinuous cyclindrical tubes grossly circular in cross-section. Tubes associated with vertisols are vertically oriented and cut across the host sediment i.e. they are strata-discordant. Continuous tubes are rare and are usually preserved as 5-10 cm long pieces. Some of them show downward bifurcations also. The surface of these tubes is smooth with some bulbous protrusions at places. The whiteness of the calcrete decreases from the core outwards in cross-section. In sections taken along the length of the calcrete a central sinuous crack/hollow is observed.

At only one site (Rayka, Mahi) such tubes were observed to distend downwards upto a level at which they spread laterally to form a mat. Here the calcrete tubes criss-cross each other and make a network. These calcretes are sandier than the tubes found associated with the vertisol. No calcrete-tubes of similar dimensions are seen in the red-soil level. Here the tubes are commonly less than half a centimetre in diameter and a few centimetres in length. Calcretes are usually 'agglutinated' with quartz particles sticking to the surface (Plate 5.17).

These calcrete tubes or rhizogenic calcretes form through the action of water uptake by plant roots which concentrates the soil water in Ca^{2+} ions, leading to supersaturation states. The rhizogenic calcretes are commonly termed as rhizoliths or root casts. Klappa (1980) introduced the term rhizolith to include "the accumulation and/or cementation around, cementation within or replacement of higher plant roots by mineral matter".

The less common distribution of rhizoliths in vertisols may be ascribed to varying degrees of hydromorphism in these soils. Since plants require oxygen to respire plant roots in water logged areas restrict their penetration and populate near surface regions only (Retallack, 1990). The vertical disposition of root casts indicates that the plants which colonised the floodplains/streams relied on perched water bodies of deeper water tables (Cohen, 1982). Consequently plants that grow in environments receiving a continuous water supply form matted root systems whereas deeper fluctuating groundwater table conditions lead to the formation of vertical rhizoliths (Cohen, 1982). The rhizolith mats observed at Rayka are of phreatophyte plants. Such plants have root systems that tap the groundwater table for their daily water needs. Phreatophytic rhizogenic calcretes have also been recorded from the Triassic (Purvis & Wright, 1991). The dominant role of plants in calcrete formation has only been recently recognised

(Rossinsky & Vanless, 1992; Wright et al., 1995) and in some cases they are the only proponents of calcrete genesis.

5 3.4 Calcrete-conglomerates

Detailed descriptions of calcrete conglomerates are given in sections 4.1 and 4.2. Here for sake of continuity the most important features of these are summarised. Most coarse-grained sediment bodies consist of calcrete as their principal clast constituents. The clast-supported conglomerates range in thickness from <0.2 m to 3 m. Trough cross-stratification and planar cross-stratification is restricted to larger bodies whereas planar stratification and non-stratified lenses are typical of smaller sediment bodies. Individual foresets are normally graded, with dips averaging around 25^0. The clast population within each foreset is divided into lower coarse clast-supported sub-stratum which 'grades' abruptly into granules of basalt and calcrete. Within the calcrete conglomerates also exist clayey-silt boulders and cobbles at the base, which are few in number. Wherever the conglomerates truncate an underlying 'vertic' clay the lower bounding surface is irregular but becomes quite planar at places. Granules of the conglomerate are seen to enter into cracks of the vertic clay. The clasts of calcrete are irregular to knobby in shape. Maximum clast size is usually 12 cm in diameter.

The trough cross-stratified facies is interpreted to have formed by the downstream migration of trains of sinuous crested dunes (Billi et al., 1987), in the deepest part of the channel. The planar cross-stratified facies represents downstream accretion of avalanching slip faces on the advancing front of a mid-channel bar. Such facies have been interpreted as representing migrating straight crested transverse bars (Clemente and Perez-Arlucea, 1993).

5.4 Calcretes: microscopic features

The calcretes of Mainland Gujarat show microscopic features that are common to the above mentioned varieties. These microscopic features are described individually and their genesis explained. The later part of this section discusses the distribution and abundance of each of these microscopic fabrics in the different types of calcretes. The present study revealed the presence of microscopic features similar to those described from all over the world such as clotted micrite, floating textures, sparitic veins and replacive and displacive fabrics.

5.4.1 Clotted micrite

Dense accumulations of equant microcrystalline calcite < 4 μm are observed in most thin sections (Plate 5.18). The micrite shows varying degrees of transmittance and is usually light brown in colour. At places microsparitic growth is common and these occur as irregularly distributed patches. Clotted micrite in most samples forms the bulk of the section. The micrite is subhedral to anhedral.

This microfabric has been reported the world over in both Pleistocene and ancient calcretes (Esteban & Klappa, 1983; Goudie, 1983; Wright & Tucker, 1991; Renaut, 1993; Tandon & Gibling, 1997). The micrite forms through the simultaneous growth of closely spaced nuclei or crystallites (Tandon & Friend, 1989) which in turn is dependent on the supersaturation threshold (Fernandez-Diaz et al., 1996). The predominance of micrite may be due to rapid carbon dioxide degassing mediated through evaporative processes. Wieder & Yaalon (1982) suggested that the presence of clays controls the size of the calcite. Greater the amount of clay smaller is the size of the micro calcite.

5.4.2 Grain coats/pendant cements

Most non-carbonate grains are enveloped by a coat of calcite (Plates 5.19, 5.20). This coat is at times of equal thickness while in some cases is thicker on one side of the grain. The calcites are usually needle-like in form but show bladed forms also. The coats are up to 8 μm thick irrespective of grain composition and shape. The coats surround clasts of quartz, feldspar, mica and heavy minerals also. At places needle calcite translates into bladed sparite. In all cases there is only one stage of crystal growth i.e. it is singly tiered. Infrequently equant sparite rim cements are also observed.

Cements mimicking grain coats are also present (Plates 5.20). The quartz grains in such situations are surrounded by multiple zones (multi-tiered) of sparite/microsparite. However the sparite is largest at the grain contact and decreases away towards the clotted micrite with which it has a sharp contact.

Grain coats are described in literature as pendant cements when asymmetrically disposed (Longman, 1980; James & Choquette, 1984; Chafetz et al., 1985; Gardner & McLaren, 1994). These are also termed as gravity cements because of the action of gravity in the formation of a bulb of water underneath the grain from which the calcite crystallises. These cements form immediately after the passage of meteoric waters through the sediment (James & Choquette, 1984) by evaporation and carbon dioxide degassing. Such microfabrics are seen in calcretes of all age groups throughout the globe (Lang et al., 1990; Wright & Tucker, 1991). Needle like crystal precipitation may have been driven by rapid degassing which resulted in high degrees of supersaturation (Given & Wilkinson, 1985). Degassing of CO_2 generates carbonate ions through the dissociation of HCO_2 making the system rich in carbonate. Elongate crystals result because the rate of precipitation along the 'c' axis is directly related to the concentration of carbonate ions. Fibrous cements may also be controlled by the faster growth rates under high flow

velocities which lead to larger reactant flux to the growing crystal (Gonzalez et al., 1992). But in the present case it appears that static flow conditions existed suggesting a more important role of degassing in controlling cement morphology.

Surprisingly through a review on cement types developed in spatially separated deposits over the world McLaren (1993) found that gravity cements were not developed at all. This according to her invalidates the consideration of this cement type as a typical vadose cement. However, in the present study grain coats are developed profusely in most thin sections suggesting that this viewpoint might be incorrect.

Grain-coat mimicking cements appear to be pore cements in channels. What one observed is a cross section of a pore throat in which a crystal of quartz has been trapped. In this case the cements would grow from the pore walls towards the grain as observed.

5.4.3 Sparitic/Microsparitic veins

Sinuous veins of calcite cut across randomly in all thin sections (Plate 5.21). These veins are filled with sparite or microsparite and is directly linked with the width of the vein which ranges between 16 μm and 72 μm. The drusy spar changes in its dimension from the walls where it is 8-12 μm to the centre of the vein where it is up to 50 μm in size. Sparitic veins occur in isolation or may contain offshoots. All veins narrow at their terminations which are usually directed towards the interior of the nodule. Sometimes the growth vectors of calcites are directed inwards from the clotted micrite wall but does not fill the vein leaving some hollow space between oppositely facing crystal face terminations. Calcite veins also contain floating micritic intraclasts and quartz grains, but such instances are few.

The sparitic/microsparitic veins are in all probability dual in origin. Those with intraclasts and large sparite growths appear to be shrinkage planes which have been

subsequently cemented by the pore-filling sparite. Such veins do not have too many offshoots. On the other hands smaller veins that are filled with microsparite and are profuse may have resulted as the filling of channels generated by rootlets and these have often been termed as crystallaria (Wright & Tucker, 1991). Sparitic veins are a common feature of all calcretes that show shrinkage features (Goudie, 1983; Tandon & Friend, 1989; Wright & Tucker, 1991; Raghavan et al., 1991)

5.4.4 Displacive & replacive fabrics

Most siliciclastic grains show evidences of etching on their margins (Plate 5.22). In sections the etching manifests itself as a continuous array of 'C' shaped connected depressions with the concave surfaces facing away from the grain. The length of these pits is not uniform which gives a corroded appearance to the grains.

Some siliciclasts contain a network of calcite veins cutting across. This creates a visual effect as if the grain had exploded (Plate 5.23). The match between boundaries of adjacent clast particles is like those in a jigsaw puzzle indicating that originally the grain was one. In other cases quartz grains are bisected by a calcite vein of a single array of microsparite. Micaceous grains show growth of calcite along the cleavage planes that causes them to bulge giving rise to an 'augen' like structure seen in gneisses.

The corrosion has been reported to be omnipresent in calcretes (Goudie, 1983; Wright & Tucker, 1991). Due to the unsaturation of the pore fluids with respect to silica the interaction of such waters with grains causes dissolution (Wang et al., 1994).

Displacive growth (exploding grains) results through evaporative processes in the vadose zone. The mechanism begins with the withdrawal of porewater from grain surfaces and segregation within inter granular boundaries along cleavage planes and inter-grain contacts (Braithwaite, 1989). Through attaining high levels of saturation calcites

grow displacive linearly. Along cleavage planes calcites enlarge as island growths causing the host micas to expand directions orthogonal to the planes. The controlling parameter for displacive growth appears to be a unique condition of supersaturated water retention exclusively in micropores. Supersaturation generates pressures that are amplified and focused through smaller grain contacts. This concentration of stresses is essential owing to the fact that calcite under no confining pressure has a strength, two orders of magnitude less than quartz (Buczynski & Chafetz, 1987). Hence the moot point is that displacive growth does not generate through the direct action of calcite on grains (siliciclasts) but by stresses transmitted through grain contacts. However, as observed in certain thin sections large grains exhibit exploding fabrics and also at the same time float in a sea of micrite. This would necessitate a direct action of calcite on quartz, rather than stress amplification through framework grains.

5.4.5 Distribution of fabrics

Grain coated calcites were observed in thin sections of rhizogenic and pedogenic calcretes. They were absent in groundwater calcretes and were less profuse in hydromorphic-soil calcretes from Mahudi (Sabarmati). These cements were well developed in cauliflower calcretes wherein each and every grain developed a coat.

Clotted micrite was present in all types except groundwater calcretes in which the sediment was passively cemented and showed larger siliciclast density. Patches of micrite were present in the core of rhizoliths. Towards the rim of the nodule the number of detritals increased. In pedogenic and hydromorphic soil calcretes and cauliflower calcretes it formed the dominant feature of the nodule.

Sparitic veins again were observed in each type but was relatively less developed in groundwater calcretes. Similar distribution of displacive and replacive textures was also seen although some grains in groundwater calcretes showed signs of corrosion.

The presence of coated grains in rhizogenic and some pedogenic carbonates and also in the enigmatic cauliflower calcretes shows that initially carbonate cementation effected in the vadose zone. With progressive occlusion of pore spaces the sediment was completely saturated with water which led to the precipitation of micrite. Through successive wet-dry cycles the intergranular clays in pedogenic and groundwater calcretes caused the formation of shrinkage cracks which ultimately formed sparite-filled veins. In rhizoliths, rootlets played a more significant role in the formation of microsparite veins. The less profuse development in hydromorphic calcretes of grain coats is self evident since in these situations the pores were already water saturated thus preventing the formation of gravity cements. A general sequence of cement stratigraphy was:

Stage 1 : Formation of pendant cements suggesting vadose conditions. This stage is absent in hydromorphic and groundwater calcretes.

Stage 2 : Precipitation of clotted micrite and formation of shrinkage cracks.

Stage 3 : Displacive growth and the development of floating grain textures.

5.5 Calcretes: Mineralogy

With a view to characterising the composition of calcretes, the carbonate rich phases within certain nodules were powdered and analysed using standard X-ray diffractometric and FT-IR techniques.

5.5.1 X-Ray diffractometry

Powdered samples were analysed with a Phillips PW 1729 CuKα source X-ray diffractometer. The scanning range taken was from 4° to 60°. Samples taken had higher

concentrations of calcium carbonate (the most white nodules) from each type described above. All the samples contained exclusively low magnesium calcite as is seen in most calcretes (Hay & Wiggins, 1980; Watts, 1980). None gave signatures of either dolomite or aragonite within them. The various peaks observed in all samples are summarised in table 5.2.

SAMPLE	212	116	108	202	113	110	104
D/RS	1.6026	1.8715	1.9103	2.0920	2.822	2.4908	3.0295
P/GW	1.6022	1.8741	1.9110	2.0927	2.2848	2.4923	3.0316
M/V1	1.6039	1.8782	1.9161	2.0975	2.2885	2.5003	3.0446
R/V3	1.5997	1.8713	1.9096	2.0897	2.2811	2.4913	3.0293
M/V2	1.5981	1.8723	1.9074	2.0900	2.2774	2.4855	3.0223
M/V3	1.6018	1.8737	1.9107	2.0928	2.2814	2.4916	3.0280
M/C	1.6008	1.8753	1.9136	2.0949	2.2855	2.4936	3.0380

Table 5.2: X-ray diffractometer peak values for various hkl planes. Values are in Angstroms Å.

5.5.2 Infra-red spectroscopy

As this technique is used less frequently than x-ray diffractometry in sedimentology the principles of it are given here.

Vibrational spectroscopy is a useful mineral-study technique that involves the analysis of the absorption behaviour of light in the infra-red region (0-10000 cm^{-1}) by vibrating molecules. In infra-red spectroscopy a distinction is usually made between the near-IR spectrum (10,000-4000 cm^{-1}), the mid-IR spectrum (4000-400 cm^{-1}) and the far-IR spectrum (400-10 cm^{-1}). The analyses of carbonate phases has been carried out in the mid infra-red region of the spectrum. Each peak in the spectrum represents vibrational transitions or in other words frequencies of the sample. As individual peaks indicate structural groups within the sample these spectra yield information regarding the occurrence of phases or molecular groups.

In any crystal or molecule only a specific number of vibrational modes are allowed and equals the number of classical degrees of vibrational freedom. In a crystal the periodic arrangement of atoms in a motif causes the vibrational modes to travel as displacement waves. These waves are termed as lattice vibrations. Depending on the orientation of nuclear displacements with respect to the wave propagation direction they may be classified as longitudinal when parallel and transverse when perpendicular.

These nuclear displacements generate an oscillating dipole moment; the frequency of the oscillating dipole wave being determined by the oscillation frequency of individual atoms and the wavelength of the associated lattice vibration. Such vibrations can interact with light and are called as `optic modes'. Again two mutually perpendicular orientations are the transverse-optic (TO) and longitudinal-optic (LO) modes.

The mid infrared spectrum of a given substance is characteristic for the mineral. Consequently the technique can be used in tandem with X-Ray diffractometry for the purpose of routine mineral identification. Additionally as per the theory outlined above for carbonate phases various structural groups like CO_3, CaO, OD, OH, structural H_2O may be identified.

Eight samples were either scraped or micro-drilled from polished specimens of calcretes. For one sample spectra were obtained for both the micritic groundmass as well as sparitic veins. The resulting detritus produced was powdered in an agate mortar and sieved through a 325 mesh sieve to collect uniform sized powder. Alkali halide pellets were prepared using a ratio of 1:15 (sample to alkali halide) with the help of a hydraulic pressing apparatus. The pellets were then analysed using a Nicolet Magna IR 550 Fourier-transform infrared spectrometer.

Since the spectra were uniform for all samples that were processed only two representative ones are reproduced (Figs. 5.2, 5.3). Absorption peak values for all samples are given in Table 5.3.

SAMPLE	H_2O stretching band	Surface adsorbed hydrous species	OD stretching vibration	CO_3^{2-} Asymmetrical stretching	CO_3^{2-} Bending mode	CO_3^{2-} bending mode
D/RS	3453	2882	2512	1430	882	712
M/12	3450	2874	2520	1426	876	717
V/C	3448	2878	2517	1423	879	714
R/V3	3450	2927	2518	1422	876	716
V/C	3447	2876	2515	1422	876	713
M/V1	3451	2927	2519	1420	876	715
M/C	3447	2926	2519	1431	878	713

Table 5.3: Absorption values for calcite with various responsible molecular group vibrations assigned. Units are in wavenumbers cm^{-1}.

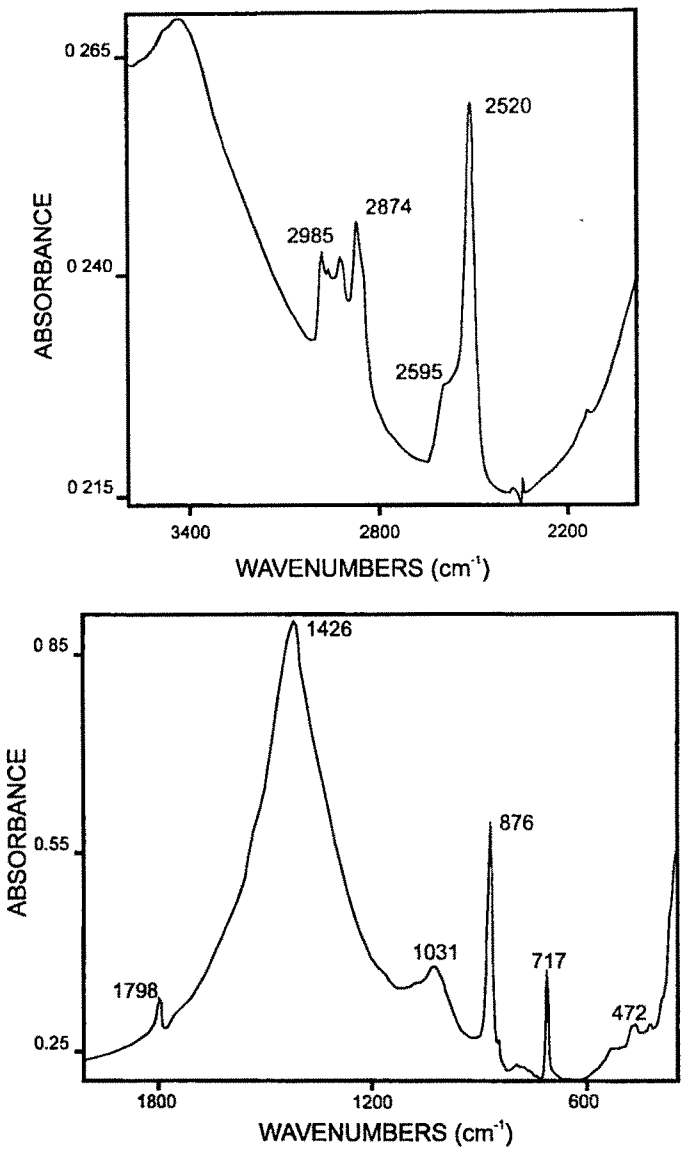

Figure 5.2: FT-IR spectra showing various absorption bands.group vibrations assigned. Units are in wavenumbers cm^{-1}. Sample = M/12.

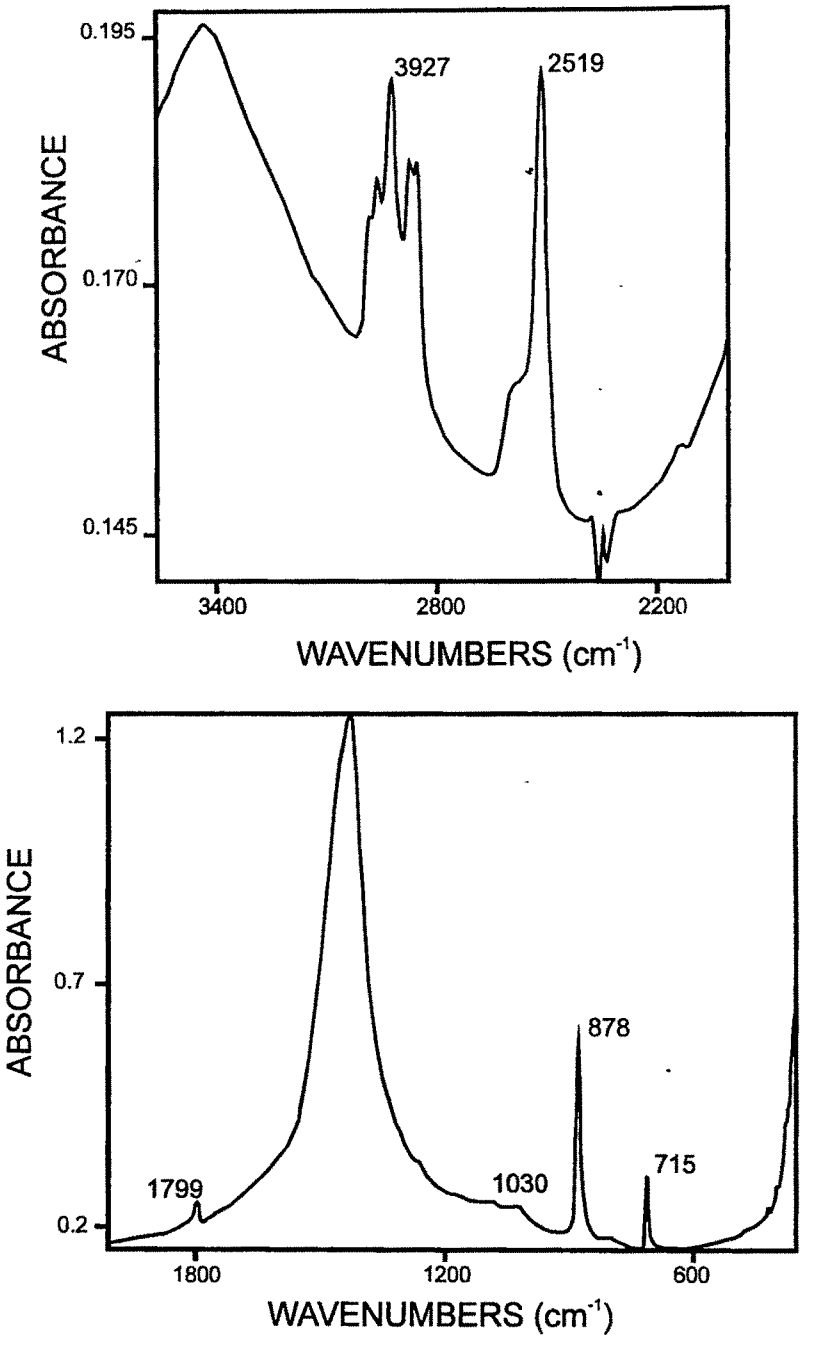

Figure 5.3: FT-IR spectra showing various absorption bands.group vibrations assigned. Units are in wavenumbers cm^{-1}. Sample = M/V1.

The purpose of the analyses was to see whether it is possible to distinguish between continental carbonates and marine carbonates/shell carbonates. Calcretes in continental interiors provide a wonderful opportunity to characterize meteoric calcites. Chemical analyses on these indicate that all of the samples are low magnesium calcites. No dolomitic admixtures are present.

The spectra show peaks characteristic of the carbonate mineral calcite which are at 1422-1431 cm^{-1} , 876-882 cm^{-1} and 712-716 cm^{-1}. The last peak is diagnostic for calcite (Lyon, 1971). The peaks around 1425 cm^{-1} correspond to the carbonate asymmetrical stretching vibration whereas those in the regions of 875 cm^{-1} and 715 cm^{-1} have been assigned to CO_3^{2-} bending modes (White, 1974). Adsorbed water stretching vibrations and those for hydrous species are seen as a broad absorption band around 3450 cm^{-1} and sharp peak at 2880-2920 cm^{1}. The only aspect in which the spectral signatures of meteoric calcites varied from the marine counterparts was the presence of a sharp absorption peak at 2500 cm^{-1}. This region of the spectrum is usually represented by absorption of OH and OD vibrations. For example the OD vibration in $Ca(OD)_2$ is at 2689 cm^{-1}, for $CaSO_4.2D_2O$ at 2650 cm^{-1} and for $Sr(OD)_2$ at 2560 cm^{-1} (Ryskin, 1974). The incorporation of the heavier hydrogen isotope in to the crystal lattice of calcite may be explained by the formative conditions of the mineral. In semi-arid regions groundwaters have consistently high deuterium levels (Bhattacharya et al., 1985). Moreover during the precipitation of calcite from meteoric waters, $\delta^{18}O$ gets preferentially incorporated into the crystal structure. Since $\delta^{18}O$ and D co-vary in the groundwaters it may be possible that the fractionation behaviour for deuterium is grossly similar to oxygen. That magnesian calcites could contain water molecules has been recognized by various workers (Mackenzie et al., 1983; Gaffey, 1988). Mackenzie et al., (1983) go on to suggest that magnesian calcites should be considered to be

a three component system of $CaCO_3$-$MgCO_3$-H_2O. The present study also supports this assertion.

5.6 Calcretes: Elemental chemistry

Pure samples of calcretes were analysed for their Mg and Sr content using X-ray fluorescence technique. Pellets were made using 5 gms of powdered sample and analysed using a Siemens 3000 machine. The magnesium values were converted to ppm values and the bivariate plot is shown in figure 5.4. It is clear from this figure that Mg and Sr co-vary linearly although the scatter is quite large. Such co-variation is due to the incorporation of Mg^{2+} ions having smaller ionic radii into the calcite lattice resulting in the expansion of Ca sites which causes increased Sr subsitution (Banner, 1994). Using X-ray absorption spectroscopy Pingitore et al., (1992) showed that once strontium is incorporated into the calcite lattice it is not mobile relative to Ca^{2+}. Hence preferential leaching of strontium during weathering does not take place.

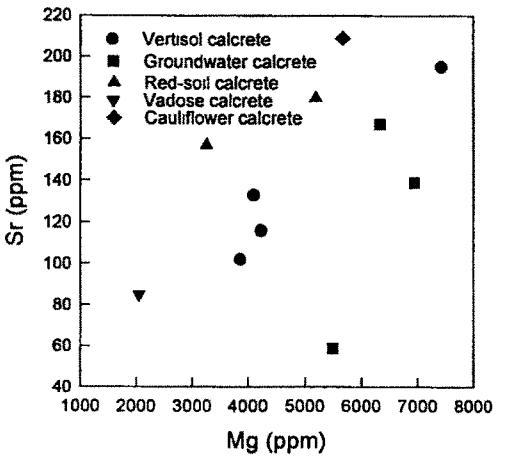

Figure 5.4: Bivariate plots of Sr vs. Mg showing covariation of both elements

Mg values range between 2000 ppm to 8000 ppm. Some samples of groundwater calcretes and vertisol calcretes show higher values. The strontium concentrations vary between 60 ppm to 220 ppm. These values are quite low. Very few studies exist on the strontium levels in calcretes. Few studies on dolocretes from Kuwait (El-Sayed et al., 1990) and Spanish dolocretes (Spötl & Wright, 1992) are available for comparisons and are plotted in figure 5.5. These comparisons show that the calcretes from Mainland Gujarat have very low concentrations. Moreover all the calcretes and dolocretes have values that are much less than marine abiotic calcites (Carpenter & Lohmann, 1992) which range between 1000 ppm to 3200 ppm.

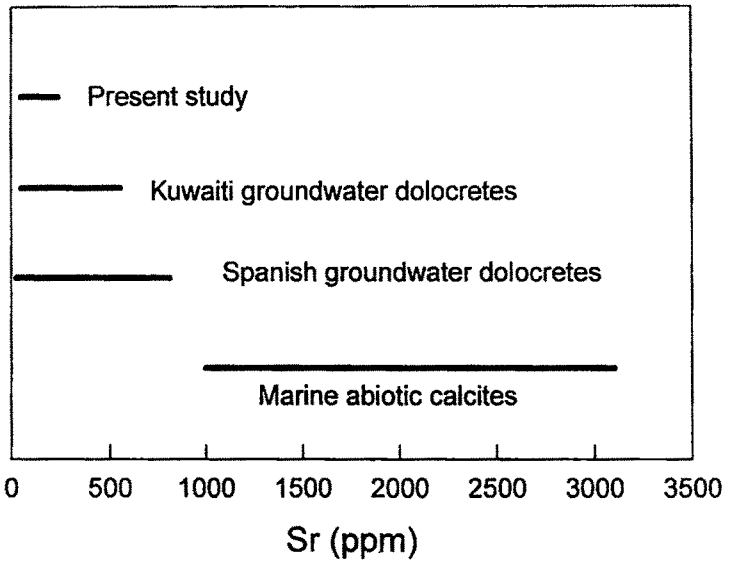

Figure 5.5: Concentration of Sr in meteoric and marine calcites. Note the large difference between the two varieties. Sources: Kuwaiti dolocretes (El-Sayed et al., 1990), Spanish dolocretes (Spötl & Wright, 1992), marine calcites (Carpenter & Lohmann, 1992).

Sr concentrations in river waters are typically in ppb levels. For the Sabarmati river Trivedi et al., (1995) reported values around 400 ppb. During evaporative concentration or rapid crystallization (Carpenter & Lohmann, 1992), which again is

related to either high evaporation rates or rapid CO_2 degassing, meteoric waters get enriched with respect to Sr and such mechanisms may explain the high values in calcrete calcites (Spötl & Wright, 1992). Such characteristic concentrations may turn out to be a useful criterion in identifying calcretes chemically.

5.7 Calcretes: Stable isotopes

Samples were cut into slabs and were micro-sampled using a rotary motorised drill. Stable isotope measurements were carried out by the conversion of calcite to carbon dioxide. This liberation of gas was done by the reaction of the sample with 100% phosphoric acid. Results are reported with respect to PDB in the standard δ (permil) notation where

$$\delta\ (‰) = [(R_{sample})/R_{standard})-1] \times 1000$$

R_{sample} and $R_{standard}$ are the $^{13}C/^{12}C$ or $^{18}O/^{16}O$ ratios in sample and standard respectively. Samples were analysed using a VG Micromass 903 mass spectrometer. The overall reproducibility of $\delta^{18}O$ was ±0.25 ‰ and for $\delta^{13}C$ ±0.1 ‰.

The samples yielded a large range in $\delta^{13}C$ values ranging between -7 ‰ to -1 ‰ whereas the range in $\delta^{18}O$ were constrained between -2.5 ‰ and -5 ‰ (Fig. 5.6). The $\delta^{18}O$ of pedogenic carbonate is in equilibrium with that of soil water whose isotopic composition is related to that of meteoric water. The isotopic composition of soil water may be significantly different in some cases owing to differential infiltration, evaporative modification and modification through evapotranspiration processes (Cerling & Quade, 1993).

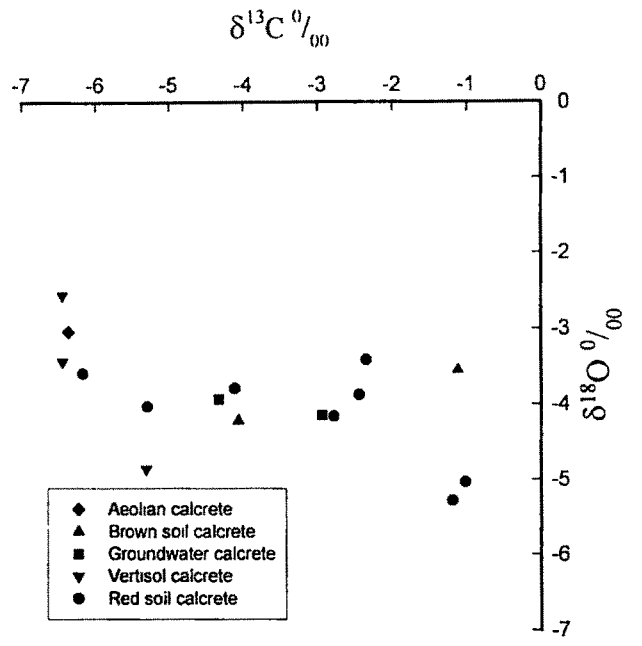

Figure 5.6: Stable isotope concentrations in calcretes. Note the absence of any covariation. The carbon isotope values are spread over a large range while oxygen isotopic values are constrained in a narrow band.

The relationship between temperature and the isotopic value of water is given by the equation:

$$1000 \ln\alpha_{c\text{-}w} = (2.78 \times 10^6 / T^2) - 2.89$$

where T is temperature in Kelvin (Friedman & O'Neil, 1977) and

$$\alpha_{c\text{-}w} = (1000+\delta^{18}O_{calcite}) / (1000+\delta^{18}O_{water})$$

Figure 5.7 gives the range of isotopic composition deduced from the above relationship for parent fluid composition for a temperature range between 20 °C to 25 °C. Also plotted is a bar that represents the modern groundwater values in Gujarat (Bhattacharya et al., 1985). A remarkable correspondence exists between these two ranges suggesting that the isotopic composition of meteoric waters has not changed remarkably during the past.

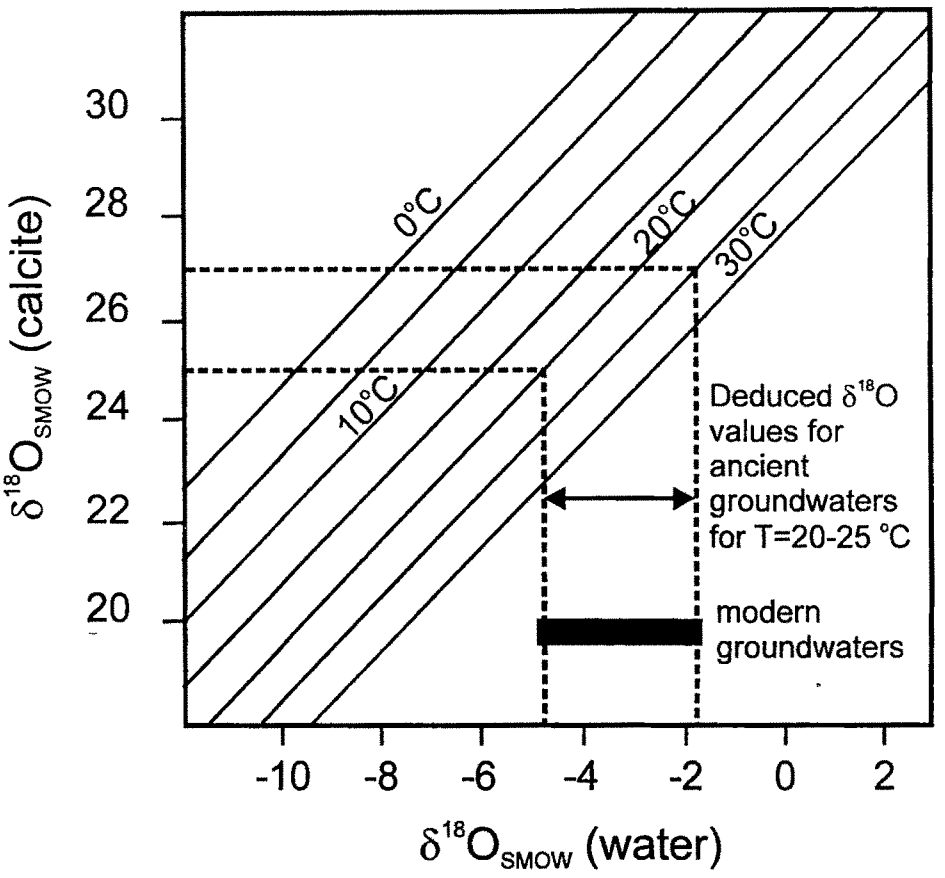

Figure 5.7: Relationship between oxygen isotope values of water and calcite. Fractionation curves were calculated from the equations in Friedman & O'Neil (1977). Black band shows values for modern groundwaters (Bhattacharya et al., 1985) which falls in the same area as estimated values (arrow) for a temperature range between 20-25 °C.

The $\delta^{13}C$ content of pedogenic carbonate is governed by the stable isotopic composition of soil carbon-dioxide which in turn is determined by the nature of the vegetation biomass. Plants may be classified on the basis of their photosynthetic pathways into C3, C4 or CAM. C3 plants utilise the Calvin cycle which involves an initial CO_2 carboxylation to form phosphoglyceric acid (3 carbon acid). The isotopic composition of such plants is -26 ‰. This class of plants include virtually all trees most shrubs, herbs and forbs. C4 plants follow the Hatch-Slack cycle wherein carbon dioxide combines with a phosphoenol pyruvate to form malate or aspartic acid (4 carbon acid).

The average isotopic composition of C4 plants is -13 ‰. Warm season grasses and sedges are the major members of this clan.

Based on a diffusion based model Cerling (1984) demonstrated that an enrichment of 14 ‰ takes place in calcite forming in soils (Cerling et al., 1991; Quade et al., 1995). Thus pedogenic calcretes forming under a C3 dominated plant cover have values near -12 ‰ while purely C4 dominated ecosystems have values of +2 ‰. In the present study calcretes associated with vertisols have negative values around -7 ‰ (PDB). If one assumes the above values as typical for C3 and C4 end members then the vertisol calcretes formed under a mixed C3-C4 ecosystem with 35 % C4 and 65 % C3 vegetation biomass. The wide range in carbon isotopic values for the red soil calcretes may be due to the presence of a largely C4 dominated vegetation with pockets of C3 vegetation (sparsely wooded shrublands or grasslands). In this case the large negative values probably reflect the isotopic composition of the sparse wooded vegetation.

5.8 Formative pathways and sinks

It is clear that calcium carbonate is present as a major deposit within the entire alluvial depositional system, as calcretes. Calcretes occur in intra-channel as well as extra-channel areas as precipitation along stratification planes. These two formative situations have been grouped as groundwater calcretes and are characterized by inorganic precipitation from laterally migrating river water/groundwater saturated with respect to carbonate. An alluvial system is rarely stable and thus prone to avulsion. Calcretized channels may consequently be abandoned at times forming banks of subsequent channels through events of extreme discharges (Malik and Khadkikar, 1996). Groundwater calcretes later are subjected to soil forming processes (Plate 5.24). This results in the redistribution of carbonate, the degree of which increases with distance from the principal

channel tract (Bown and Kraus, 1987). In contrast, as in case of a rapidly subsiding basin such groundwater calcretes may be preserved in their original form often escaping any pedogenic modification. Pedogenesis of the sediments containing groundwater calcretes leads to the development of pedogenic calcretes. Once formed soil calcretes may be permanently arrested or in turn may be remobilized. This remobilization is facilitated by fluctuating river discharges or meandering channels which leads to instantaneous bank scouring. Underscouring and bank collapse causes large loads of sediments to fall within the channel. In the present case calcretes are released in large amounts to form the calcrete-conglomerates. Calcrete conglomerates observed at the same level as the vertic pedogenic calcretes are rich in calcrete clasts. This may be ascribed to the swelling character of smectitic clays of the soil. The clays absorb large quantities of river water making them swell, causing the soil to be more cohesive and homogenous thus preventing its erosion. Protruding calcretes however can be easily plucked out by strong currents from the bank surface causing large concentration of this material within the channel. Alternatively, the compositional homogeneity of calcrete-conglomerates may be due to sorting of bank debris on account of different entrainment velocities of soil silt/clay and calcrete pebbles/cobbles. The presence of large mud clast indicates bank-collapse to be a significant process. The flow diagram in figure 5.8 summarizes the above processes.

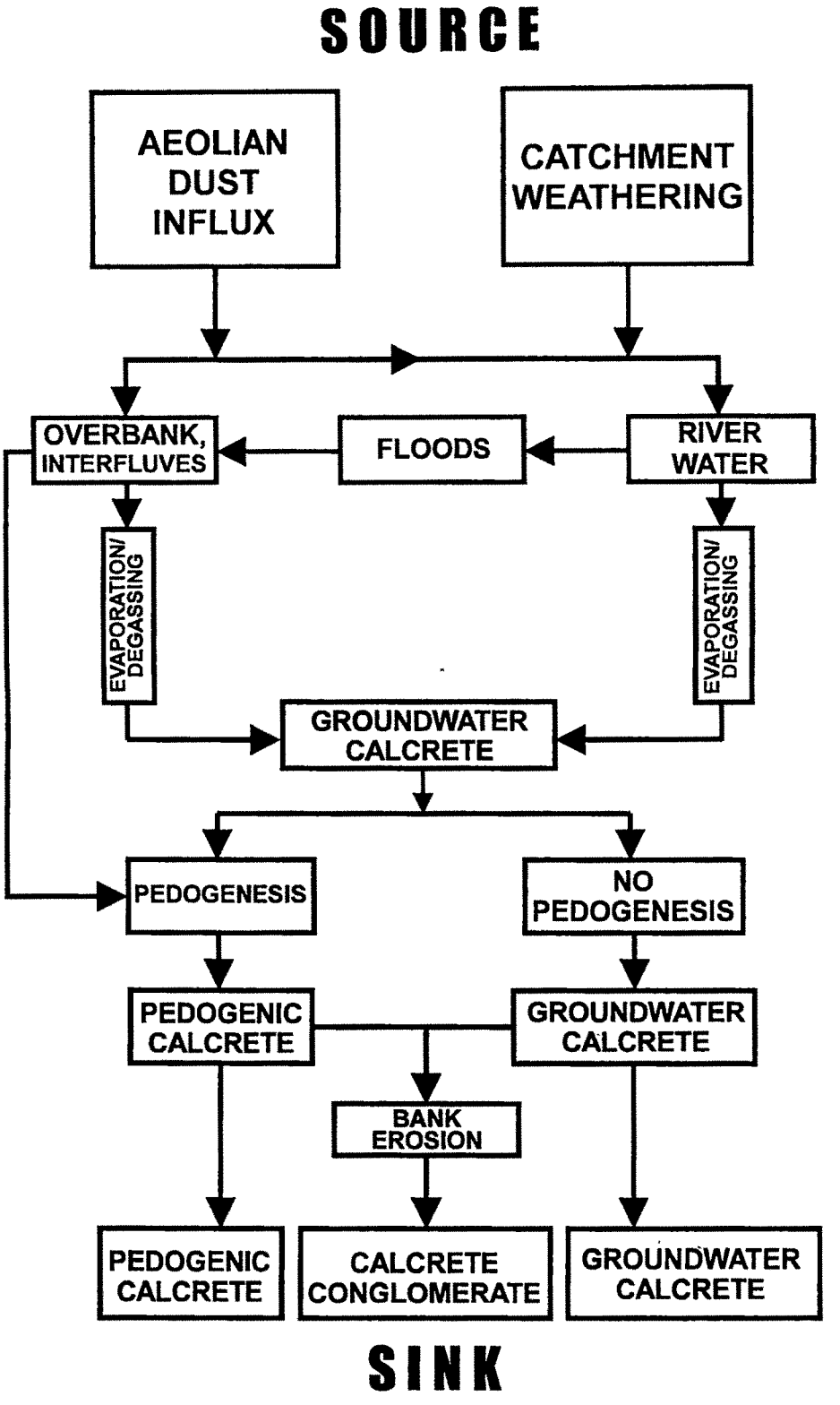

Figure 5.8: Formative pathways and sinks in semi-arid to sub-humid alluvial systems (Khadkikar et al., 1998).

The pathways that lead to the three sinks has considerable implications on 1) morphogenetic sequences of pedogenic calcretes (Gile et al., 1966) observed in soils and 2) carbonate source for arid zone soils. Conventionally, aeolian dust is believed to be a major source of carbonate in arid zones (McFadden, 1988). While it is true that aeolian dusts do contribute towards the soil carbonate budget, the presence of extensive groundwater calcretes in the host sediments suggests an additional route through carbonate-saturated river waters (Zaleha, 1997; Khadkikar et al., 1998). River waters again, may receive carbonate either through catchment weathering or aeolian dust. Zaleha (1997) documented laminated mudstones from the Siwalik succession of Pakistan which contained more than 10 % calcite. These calcites he argued could be 1) allochthonous detrital grains, 2) detrital carbonate grains precipitated from flood waters or 3) cement from floodwaters. For floodwaters to deposit 0.1-0.2 cm sediment per unit area with 17 % calcite by weight requires suspended sediment concentration on the order of 0.186 gml^{-1} and water depths around 0.5-1.4 m (Zaleha, 1997). Such conditions require that areas of calcite precipitation be low topographic areas in the floodbasin if at all calcium carbonate is to be concentrated.

A study of calcretes sampled progressively up-profile from groundwater calcretes beyond the influence of the soil till the vertisol was carried out. Sheets of groundwater calcretes that once are continuous become discontinuous (Plate 5.25). The sheets begin to segregate upwards into nodular masses that are smooth topped and popcorn like in appearance. These popcorn calcretes translate upwards into 5-10 cm large disorthic nodules. Petrographic examination shows an absence of displacive or replacive growths in the pure groundwater calcretes. Passive cementation by microsparite with large grain densities are seen. In the transitionary stage micritic patches begin to appear and inter-grain distances begin to enlarge. Sparitic veins are also seen which suggest shrinkage

processes and the displacive introduction of calcium carbonate. In the proper pedogenic calcretes all the microfabrics such as clotted micrite, displacive and replacive textures, sparitic veins and floating grain fabrics are seen. It is visualised that the sediment before pedogenesis was all calcretized through groundwater processes forming bands of calcium carbonate as seen in non-pedogenised channel fill deposits. Through progressive pedogenesis this carbonate was mobilised and added on to the groundwater calcretes causing the formation of clotted micrites. With increase in the authigenic montmorillonite content shrink-swell processes gained dominance which led to the fragmentation of the sheets. This coupled with repeated dissolution-reprecipitation caused the development of the pedogenic calcretes.

Since in alluvial systems considerable amount of carbonate is already present as groundwater calcretes, nodule formation would be greatly accelerated leading to faster accretion rates and probably larger nodule sizes. In the present case upto 10 cm sized disorthic nodules have been observed. This could lead to some misjudgement regarding the maturity of the soil derived on the basis of the morphogenetic sequences (Gile et al., 1966; Machette, 1985). A similar observation has also been recently made by Slate et al., (1996) in their study of hydromorphic soils. They rightly point out that soil-carbonates that form under the influence of a shallow groundwater table may reach large dimensions (Kraus & Aslan, 1993) leading to erroneous interpretations on soil-maturity and warn against the usage of such calcretes for palaeoenvironmental interpretations. These studies are on soils that are influenced by groundwater *during* their formation. Calcic palaeosols in the Pakistan Siwaliks on the other hand as in the present case form preferentially on substrates where syndepositional calcite precipitation has occurred prior to pedogenesis (Zaleha, 1997). The present study highlights that such large dimensions can also be

attained by soils developing over sediments that have undergone groundwater calcretization.

5.9 Calcrete semantics

5 9.1 Introduction

Definitions are prone to change as science evolves. Hence it is out of necessity that at times an introspection is taken of the subject, after years of intense research. Here calcrete semantics are examined in light of new finds and old ones too. The theme thus pertains to processes, products and the definition of calcrete. In this section, in no way is a comprehensive review attempted. It is our present understanding of calcretes that is taken a cognisance of, the appropriateness of the definition of calcrete examined and a new definition proposed.

In the 'Introduction' the definitions of calcrete were introduced. For sake of continuity the same definitions are repeated here. Goudie (1972) defined calcrete as:

'A term for terrestrial materials composed dominantly but not exclusively of calcium carbonate which occurs in states ranging from powdery to nodular to highly indurated and involve the cementation of, accumulation in and/or replacement of greater or lesser quantities of soil, rock or weathered materials primarily in the vadose zone. It does not however embrace cave deposits (speleothems), spring deposits (for which tufa or travertine are accepted terms), marine deposits (such as beachrock) or lacustrine algal stromatoliths'.

This definition takes into consideration the macroscopic charcters of calcretes but ignores mineralogical variations. It also implicitly denies inclusion of calcium carbonate precipitated in phreatic zones.

Klappa (1983) defined calcrete as an accumulation of predominantly fine-grained low magnesium calcite having formed within the meteoric vadose zone by pedodiagenetic alteration and replacement of any precursor host material.

Here again there is a stress on including only those carbonates that form in the vadose zone under the influence of the soil profile. Phreatic calcretes and hydromorphic calcretes again are excluded.

The most recent definition proposed is by Wright & Tucker (1991) that has gathered widespread acceptability and states:

"Calcrete is a near surface, terrestrial accumulation of predominantly calcium carbonate, which occurs in a variety of forms from powdery to nodular to highly indurated. It results from the cementation and displacive and replacive introduction of calcium carbonate into soil profiles, bedrock and sediments in areas where vadose and shallow phreatic groundwaters become saturated with respect to calcium carbonate."

This definition recognizes that calcretes also form in phreatic conditions in a variety of substrates but ignores the role of vegetation (ditto for all early definitions) or rhizogenic activity in concentrating calcium carbonate.

The question then arises whether or not all aspects of calcrete are incorporated in the definition. Should the definition include only macroscopic characters or should diagnostic microfabrics and chemical fingerprints (if any) be included to assist in recognition of calcrete when examined at all scales.

5.9 2 Characters of calcretes

In this section the various attributes of calcretes at different spatial scales are summarised (which inevitably will involve repeating what has already been discussed in earlier sections) that affect the way calcrete may be defined in the future.

Macromorphology:

Calcrete occurs in a wide range of forms (Reeves, 1976; Netterberg, 1980). This has been well demonstrated by Netterberg (1980) who documented a range from calcified soil to powder calcrete- (silt sized carbonate) to nodular (more common form) to brecciated bouldery calcretes. Sheets of calcrete are seen where groundwater is a major medium while pedogenic calcretes show the range described above (Present study). Pedogenic calcretes commonly have sharp boundaries with the host sediment whereas groundwater calcretes are more often than not diffuse (Khadkikar et al., 1998).

A most obvious form of calcrete that has been recorded by many workers is the rhizolith (Klappa, 1980; Cohen, 1982; Jones & Ng, 1988). This is associated with both pedogenic and groundwater calcretes. Its contribution in certain areas is so significant that Wright et al., (1995) suggest that the term 'rhizogenic calcrete' be adopted to include calcretes exclusively forming through root action. However rhizoliths do not find any mention in any of the previous definitions.

Micromorphology:

Calcretes show several features that typify them on a petrographic scale which are exemplified through the present study. These may well be used in identifying calcretes in cores. The characters include floating textures, alveolar septal textures, displacive grain breakage, siliciclastic grain corrosion, circum granular calcite, micritic groundmass and sparitic veins. In the past decade the microbial contribution to calcrete formation has been appreciated as a significant route of mineral-carbonate formation in pedogenic calcretes (Verrecchia & Verrecchia, 1994; Jones, 1988). Evidences of such activity include needle fibre calcite (Jones & Kahle, 1993; Verrecchia & Verrecchia, 1994) and calcispheres (Jones & Ng, 1988).

Again, in some locations such fabrics make up the bulk of the calcrete nodule. Such features do not find mention in any of the previous definitions of calcrete.

Mineralogy and chemistry:

Though the bulk of calcretes contain low magnesium calcite as the major mineral phase, in coast-proximal areas as well as desert interiors, calcrete may attain high levels of Mg so as to form dolomite, whereupon they may be classified as dolocretes. Talma & Netterberg (1983) summarised the range of isotopic values for Quaternary calcretes and concluded that they characteristically show $\delta^{13}C$ values between -12 ‰ to +4 ‰ and -9 ‰ to +3 ‰ for $\delta^{18}O$. They pointed out that these values were typical of calcretes and helped in distinguishing them from marine carbonates. Strontium contents of calcretes and dolocretes show a range from 50 ppm to up to 1000 ppm which still is less than concentrations in marine abiotic calcites. Magnesium varies quite a lot from as less than 0.5 % to as much as 13 %.

5.9.3 Proposed definition

From the above account it is clear that several crucial parameters have not been included in the definition of calcrete although most of them were already recorded by early workers to be significant. Though not specifically addressed above, cryogenic calcretes form another interesting facet that have recently been reported by Vogt (1989). However such case studies are few in number. Calcretes form under a wide range of mean annual rainfalls spanning from 100 mm to 700 mm (Retallack, 1994). Taking into consideration all these facets of calcretes the following definition is proposed which adds upon the Wright & Tucker (1991) definition:

Calcrete is a near surface accumulation of predominantly calcium-carbonate. It ranges in form from powdery to noduler states to boulders. It forms through the passive and/or replacive and/or displacive introduction of calcium carbonate into soil, sediment or bedrock. It forms through pedogenic and/or rhizogenic and/or groundwater and/or microbial processes in the vadose and phreatic zones of regions experiencing a mean annual rainfall between 50-700 mm. It shows typical microfabrics such as clotted micrite, alveolar septal structure, spar filled sinuous cracks, circum-granular cracks, floating siliciclastic grains, grain coating cement, exploded framework grains and needle fibre calcite and exhibits a $\delta^{18}O$ composition ranging from -9 ‰ to +3 ‰ and a $\delta^{13}C$ content between -12 ‰ to +2 ‰.

References

Ahmad, N. (1983). Vertisols *In* Pedogenesis and soil taxonomy. 2. The soil orders (Eds., L.P. Wilding, N.E. Smeck & G.F. Hall), *Elsevier Science, Amsterdam*, 91-123.

Alonso Zarza, A.M., Calvo, J.P. & del Cura, G., (1992). Palustrine sedimentation and associated features-grainification and pseudo-microkarst-in the Middle Miocene (Intermediate unit) of the Madrid Basin, Spain. *Sedimentary Geology*, 76, 43-61.

Arakel, A.V. & McConchie, D. (1982). Classification and genesis of calcrete and gypsite lithofacies in palaeodrainage systems of inland Australia and their relationship to carnotite mineralization. *Journal of Sedimentary Petrology*, 52, 1149-1170.

Arakel, A.V. (1986). Evolution of calcrete in palaeodrainages of the Lake Napperby area, central Australia. *Palaeogeography, Palaeoclimatology, Palaeoecology*, 54, 283-303.

Banner, J.L. (1994). Application of the trace element and isotope geochemistry of strontium to studies of carbonate diagenesis. *Sedimentology*, 42, 805-824.

Bhattacharya, S.K., Gupta, S.K. & Krishnamurthy, R.V. (1985). Oxygen and hydrogen isotopic ratios in groundwaters and river waters from India. *Proceedings of the Indian Academy of Sciences, Earth and Planetary Science*, 94, 283-295.

Billi, P., Magi, M & Sagri, M. (1987). Coarse-grained low sinuosity river deposits: examples from Plio-Pleistocene Valdarno Basin, Italy. *In* Recent Developments in Fluvial Sedimentology (Eds., F.G. Ethridge, R.M. Flores & M.D. Harvey), *Society of Economic Palaeontologists & Mineralogists Special Publication*, 39, 197-203.

Bown, T.M. & Kraus, M.J. (1987). Integration of channel and floodplain suites, I. Developmental sequence and lateral relations of alluvial paleosols. *Journal of Sedimentary Petrology*, 57, 587-601.

Braithwaite, C.J.R. (1989). Displacive calcite and grain breakage in sandstones. *Journal of Sedimentary Petrology*, 59, 258-266.

Buczynski, C. & Chafetz, H.S. (1987). Siliciclastic grain breakage and displacement due to carbonate crystal growth: an example from the Lueders Formation (Permian) of north-central Texas, U.S.A. *Sedimentology*, 34, 837-843.

Carpenter, S.J. & Lohmann, K.C. (1992). Sr/Mg ratios of modern marine calcite: Empirical indicators of ocean chemistry and precipitation rate. *Geochimica et Cosmochimica Acta*, 56, 1837-1849.

Cerling, T.E. & Quade, J. (1993). Stable carbon and oxygen isotopes in soil carbonates. In Continental indicators of climate (Eds., P. Swart, J.A. McKenzie & K.C. Lohmann), *American Geophysical Monograph*, 78, 217-231.

Cerling, T.E. (1984). The stable isotopic composition of modern soil carbonate and its relationship to climate. *Earth and Planetary Science Letters*, 71, 229-240.

Cerling, T.E., Solomon, D.K., Quade, J. & Bowman, J.R. (1991). On the isotopic composition of carbon in soil carbon dioxide. *Geochimica et Cosmochimica Acta*, 55, 3403-3405.

Clemente, P. & Perez-Arlucea, M. (1993). Depositional architecture of the Cuerda Delpozo formation, lower Cretaceous of the extensional Cameros Basin, North-central Spain. *Journal of Sedimentary Petrology*, 63, 437-452.

Cohen, A.S. (1982). Palaeoenvironments of root casts from the Koobi Fora Formation, Kenya. *Journal of Sedimentary Petrology*, 52, 401-414.

Coulombe, C.E., Wilding, C.P. & Dixon, J.B. (1996). Overview of vertisols: Characteristics and impacts on society. *Advances in Agronomy*, 57, 289-375.

Caudill, M.R., Driese, S.G. & Mora, C.I. (1996). Preservation of a paleo-vertisol and an estimate of late Mississippian paleoprecipitation. *Journal of Sedimentary Research*, 66, 58-70.

Driese, S.G. & Mora, C.I. (1993). Physico-chemical environment of pedogenic carbonate formation in Devonian vertic palaeosols, central Appalachians, U.S.A. *Sedimentology*, 40, 199-216.

El-Sayed, M.I., Fairchild, I.J. & Spiro, B. (1991). Kuwaiti dolocrete: petrology, geochemistry and groundwater origin. *Sedimentary Geology*, 73, 59-75.

Esteban, M. & Klappa, C.F. (1983). Subaerial exposure. *In* Carbonate depositional environments (Eds., P.A. Scholle, D.G. Bebout & C.H. Moore), *American Association of Petroleum Geologists Memoir*, 33, 1-54.

Fernandez-Diaz, L., Putnis, A., Prieto, M. & Putnis, C. (1996). The role of magnesium in the crystallization of calcite and aragonite in a porous medium. *Journal of Sedimentary Research*, 66, 482-491.

Friedman, I. & O'Neil, J.R. (1977). Compilation of stable isotope fractionation factors of geochemical interest. *In* Data of Geochemistry (Ed., M. Fleischer), *United States Geological Survey Professional Paper*, 440-KK, 1-12.

Gaffey, S.J. (1988). Water in skeletal carbonates. *Journal of Sedimentary Petrology*, 58, 397-414.

Gardner, R.A.M. & Pye, K. (1981). Nature, origin and significance of red coastal and desert dune sands. *Progress in Physical Geography*, 5, 514-534.

Gardner, R.A.M. & McLaren, S.J. (1994). Variability in early vadose carbonate diagenesis in sandstones. *Earth Science Reviews*, 36, 27-35.

Gile, L.H., Peterson, F.F. & Grossman, R.B. (1966). Morphology and genetic sequences of carbonate accumulation in desert soils. *Soil Science*, 101, 347-360.

Given, K.R. & Wilkinson, B.H. (1985). Kinetic control of morphology, composition and mineralogy of abiotic sedimentary carbonates. *Journal of Sedimentary Petrology*, 55, 109-119.

Gonzalez, L.A., Carpenter, S.J. & Lohmann, K.C. (1992). Inorganic calcite morphology: roles of fluid chemistry and fluid flow. *Journal of Sedimentary Petrology*, 62, 382-399.

Goudie, A. (1972). On the definition of calcrete deposits. *Zeitschrift für Geomorphologie*, 16(4), 464-468.

Goudie, A.S. (1983). Calcrete. *In* Chemical sediments and geomorphology (Eds., A.S. Goudie, & K. Pye). *Academic Press, London*, 93-131.

Hay, R.L. & Wiggins, B. (1980). Pellets, ooids, sepiolite and silica in three calcretes of the southwestern United States. *Sedimentology*, 27, 559-576.

James, N.P. & Choquette, P.W. (1984). Diagenesis 9 - Limestones - the meteoric diagenetic environment. *Geoscience Canada*, 11, 161-194.

Jenny, H. (1941). Factors of soil formation. *McGraw-Hill, New York*, 281 p.

Jones, B. & Kahle, C.F. (1993). Morphology, relationship, and origin of fiber and dendrite calcite crystals. *Journal of Sedimentary Petrology*, 63, 1018-1031.

Jones, B. & Ng, K. (1988) The structure and diagenesis of rhizoliths from Cayman Brac, British West Indies. *Journal of Sedimentary Petrology*, 58, 457-467.

Jones, B. (1988). The influence of plants and microorganisms on diagenesis in caliche: Example from the Pleistocene Ironshore Formation on Cayman Brac, British West Indies. *Bulletin of Canadian Petroleum Geology*, 36, 191-201.

Khadkikar, A.S., Merh, S.S., Malik, J.N. & Chamyal, L.S. (1998). Calcretes in semi-arid alluvial systems: formative pathways and sinks. *Sedimentary Geology*, 116, 251-260.

Klappa C.F. (1980). Rhizoliths in terrestrial carbonates: classification, recognition, genesis, and significance. *Sedimentology*, 27, 613-629.

Klappa, C.F. (1983). A process-response model for the formation of pedogenic calcretes. *In* Residual deposits (Ed., R.C.L. Wilson), *Geological Society London Special Publication*, 11, 211-220.

Kraus, M.J. & Aslan, A. (1993). Eocene hydromorphic paleosols: significance for interpreting ancient floodplain processes. *Journal of Sedimentary Petrology*, 63, 453-463.

Lang, J., Mahdoubi, M.L. & Pascal, A. (1990). Sedimentation-calcrete cycles in the Mesozoic Red Foramtion from central High Atlas (Telonet area), Morocco. *Palaeogeography, Palaeoclimatology, Palaeoecology*, 81, 71-93.

Longman, M.W. (1980). Carbonate diagenetic textures from nearsurface diagenetic environments. *American Association of Petroleum Geologists Bulletin*, 64, 461-487.

Lynne, W. & Williams, D. (1992). The making of a vertisol. *Soil Survey Horizons*, 33, 45-50.

Machette, M.N. (1985). Calcic soils of the southwestern United States. *Geological Society of America, Special Paper* 203, 1-21.

Mack, G.H., James, C.W. & Monger, C.H. (1993). Classification of paleosols. *Geological Society of America Bulletin*, 105, 129-136.

Mackenzie, F.T., Bischoff, W.D., Bishop, F.C., Loijens, M., Schoonmaker, J. & Wollast, R. (1983). Magnesian calcites: low temperature occurrence, solubility and solid solution behaviour. *In* Carbonates: Mineralogy and chemistry (Ed. R.J. Reeder). *Reviews in Mineralogy*, 11, 97-144.

Malik, J.N. & Khadkikar, A.S. (1996). Palaeoflood analysis of channel fill deposits. Central Tapi river basin, India. *Zeitschrift fur Geomorphogie*, 106: 99-106.

Malik, J.N., Khadkikar, A.S., Chamyal, L.S. and Merh, S.S. (1998). Late Quaternary continental sedimentation in the Mahi Basin, Gujarat, Western India. *Journal of the Geological Society of India*, communicated.

McFadden, L.D. (1988). Climatic influences on rates and processes of soil developments in Quaternary deposits of southern California. *Geological Society of America Special Paper* 216, 153-177.

McLaren, S.J. (1993). Use of cement types in the palaeoenvironmental interpretation of coastal aeolianite sequences. *In* The dynamics and environmental context of aeolian sedimentary systems (Ed. K. Pye*). Geological Society Special Publication* 72, 235-244.

Netterberg, F. (1980). Geology of southern African calcretes: 1. Terminology, description, macrofeatures, and classification. *Transactions of the Geological Society of South Africa*, 83, 255-283.

Netterberg, F. (1969). The interpretation of some basic calcrete types. *South African Archaeological Bulletin*, 24, 117-122.

Netterberg, F. (1974). The interpretation of some basic calcrete types. *South African Archaeological Society*, 2, 20-24.

Pimentel, N.L., Wright, V.P. & Azevedo, T.M. (1996). Distinguishing early groundwater alteration effects from pedogenesis in ancient alluvial basins: examples from the Palaeogene of southern Portugal. *Sedimentary Geology*, 105, 1-10.

Pingitore, N.E. Jr., Lytle, F.W., Davies, B.M., Eastman, M.P., Eller, P.G. & Larson, E.M. (1992). Mode of incorporation of Sr^{2+} in calcite: Determination by X-ray abosrption spectroscopy. *Geochimica et Cosmochimica Acta*, 56, 1531-1538.

Purvis, K. & Wright, V.P. (1991). Calcretes related to phreatophytic vegetation from the Middle Triassic Otter Sandstone of south west England. *Sedimentology*, 38, 539-551.

Pye, K. (1983). Red beds. *In* Chemical sediments and geomorphology (Eds., A.S. Goudie & K. Pye), *Academic Press, London*, 227-263.

Quade, J., Cater, J.M.L., Ojha, T.P., Adam, J. & Harrison, T.M. (1995). Late Miocene environmental change in Nepal and the northern Indian subcontinent: Stable isotopic evidence from paleosols. *Geological Society of America Bulletin*, 107, 1381-1397.

Raghavan, H., Gaillard, C. & Rajaguru, S.N. (1991). Genesis of calcretes from the calc-pan site of Singi Talav near Didwana, Rajasthan, India - a micromorphological approach. *Geoarchaeology*, 6, 151-168.

Reeves, Jr. C.C. (1976). Caliche: Origin, classification, morphology and uses. *Estacado Books, Lubbock*, 233 p.

Renaut, R.W. (1993). Zeolitic diagenesis of late Quaternary fluviolacustrine sediments and associated calcrete formation in the Lake Bogoria Basin, Kenya Rift Valley. *Sedimentology*, 40, 271-301.

Retallack, G.J. (1990). Soils of the past: an introduction to palaeopedology. *Unwin Hyman, London*, 520 p.

Retallack, G.J. (1994). The environmental factor approach to the interpretation of paleosols. *In* Factors of soil formation, a fiftieth anniversary retrospective (Eds., R. Amundson, J. Harden & M. Singer). *Soil Science Society of America Special Publication*, 33, 31-64.

Rossinsky, V. Jr. & Vanless, H.R. (1992). Topographic and vegetative controls on calcrete formation, Turks and Caicos Islands, British West Indies. *Journal of Sedimentary Petrology*, 40, 271-301.

Ryskin, Y.I. (1974). The vibrations of protons in minerals: hydroxyl water and ammonium. *In* The infrared spectra of minerals (Ed., V.C. Farmer), *Mineralogical Society Monograph*, 4, 137-182.

Sareen, B.K. & Tandon, S.K. (1995). Petrology, micromorphology and granulometry of mid to late Quaternary continental deposits of the semi-arid Sabarmati Basin, Western India. *In* Quaternary Environments and Geoarchaeology of India (Eds., S. Wadia, R. Korisettar & V.S. Kale). *Memoir, Geological Society of India*, 32, 258-276.

Schmalz, R.F. (1968). Formation of red beds in modern and ancient deserts. Discussion. *Geological Society of America Bulletin*, 79, 277-280.

Slate, J.L., Smith, G.A., Wang, Y. & Cerling, T.E. (1996). Carbonate-paleosol genesis in the Plio-Pleistocene St. David Formation, southeastern Arizona. *Journal of Sedimentary Research*, 66(A), 85-94.

Smith, R.M.H. (1990). Alluvial paleosols and pedofacies sequences in the Permian lower Beaufort of the southwestern Karoo Basin, South Africa. *Journal of Sedimentary Petrology*, 60, 258-276.

Soil Survey Staff (1975). Soil taxonomy. Handbook no. 436, Soil conservation service, *United States Department of Agriculture*.

Spötl, C. & Wright, V.P. (1992). Groundwater dolocretes from the Upper Triassic of the Paris Basin, France: a case study of an arid, continental diagenetic facies. *Sedimentology*, 39, 1119-1136.

Talma, A.S. & Netterberg, F. (1983). Stable isotope abundances in calcretes. *In* Residual deposits (Ed., R.C.L. Wilson), *Geological Society London Special Publication*, 11, 221-233.

Tandon, S.K. & Friend, P.F. (1989). Near surface shrinkage and carbonate replacement processes, Aran Cornstone Formation, Scotland. *Sedimentology*, 36, 1113-1126.

Tandon, S.K. & Gibling, M.R. (1997). Calcretes at sequence boundaries in Upper Carboniferous cyclothems of the Sydney Basin, Atlantic Canada. *Sedimentary Geology*, 112, 43-67.

Trivedi, J.R., Pande, K., Krishnaswami, S & Sarin, M.M. (1995). Sr isotopes in rivers of India and Pakistan: A reconnaissance study. *Current Science*, 69, 171-178.

Verrecchia, E.P. & Verrecchia, K.E. (1994). Needle-fiber calcite: A critical review and a proposed classification. *Journal of Sedimentary Research*, A64, 650-664.

Vogt, T. (1989). Croûtes calcaires d'origine cryogénique. *Zeitschrift fur Geomorphogie*, 75, 115-135.

Walker, T.R. (1967). Formation of red beds in modern and ancient deserts. *Geological Society of America Bulletin*, 78, 917-920

Wang, Y., Nahon, D. & Merino, E. (1994). Dynamic model of the genesis of calcretes replacing silicate rocks in semi-arid regions. *Geochimica, Cosmochimica Acta*, 58, 5131-5145.

Watts, N.L. (1980). Quaternary pedogenic calcretes from the Kalahari (southern Africa): mineralogy, genesis and diagenesis. *Sedimentology*, 27, 661-686.

White, W.B. (1974). The carbonate minerals. *In* The infrared spectra of minerals (Ed., V.C. Farmer), *Mineralogical Society Monograph*, 4, 137-182.

Wieder, M. & Yaalon, D.H. (1974). Effect of matrix composition on carbonate nodule crystallization. *Geoderma*, 11, 203-220.

Wieder, M. & Yaalon, D.H. (1982). Micromorphological fabrics and developmental stages of carbonate nodular forms related to soil characteristics. *Geoderma*, 28, 203-220.

Wilding, L.P. & Tessier, D. (1988). Genesis of vertisols: shrink-swell phenomena. *In* Vertisols: their distribution, properties, classification and management (Eds., L.P. Wilding & R. Puentes), *Technical Monograph, Texas A&M Printing Centre*. 18, 55-81.

Wright, V.P. & Tucker, M.E. (1991). Calcretes: an introduction. *In* Calcretes (Eds., V.P. Wright & Tucker, M.E.). *International Association of Sedimentologists Reprint Series*, 2, 1-22.

Wright, V.P., Platt, N.H., Marriott, S.B. & Beck, V.H. (1995). A classification of rhizogenic (root-formed) calcretes, with examples from the Upper Jurassic-Lower Cretaceous of Spain and Upper Cretaceous of southern France. *Sedimentary Geology*, 100, 143-158.

Yaalon, D.H. & Kalmar, D. (1978). Dynamics of cracking and swelling clay soils. Displacement of skeleton grains, optimum depth of slickensides, and rate of intra-pedonic turbation. *Earth Surface Processes and Landforms*, 3, 31-42.

Zaleha, M. (1997). Siwalik paleosols (Miocene, northern Pakistan): genesis and controls on their formation. *Journal of Sedimentary Research*, 67, 821-839.

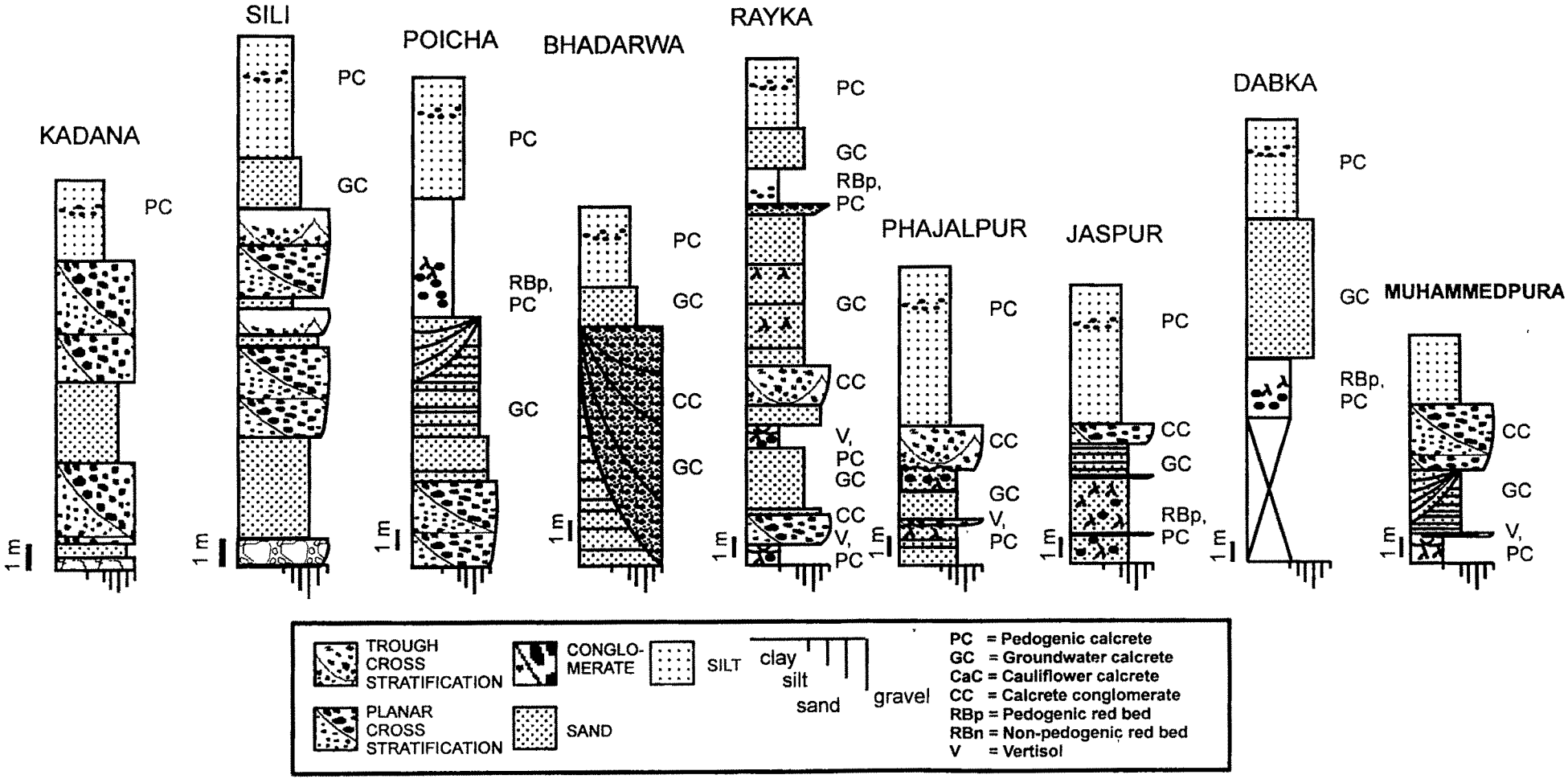

Plate 5.1: Lithologs of the Mahi basin showing distribution of calcretes and palaeosols

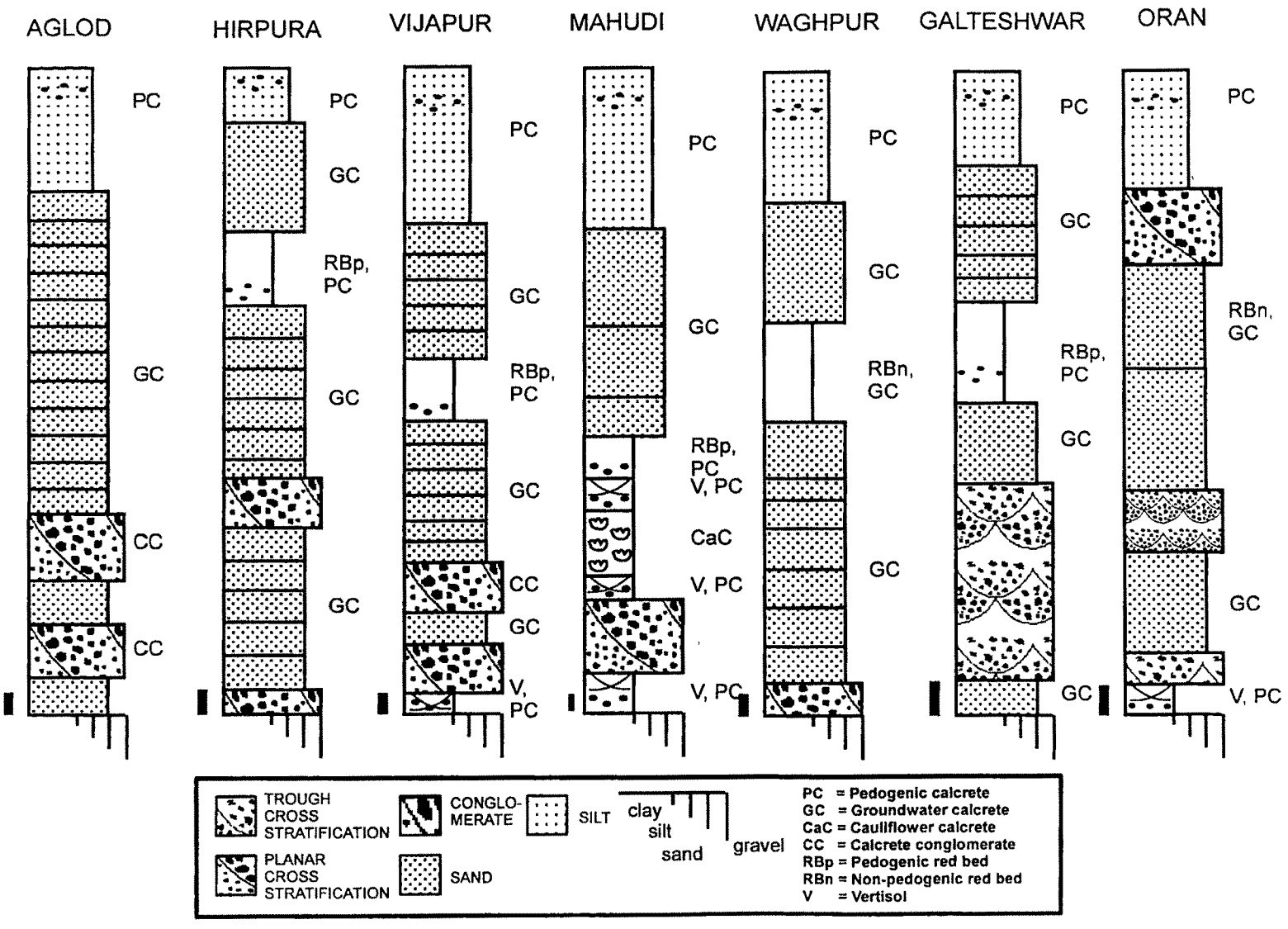

Plate 5.1 (contd.): Lithologs of the Sabarmati basin showing distribution of calcretes and palaeosols

Plate 5.2: Pseudo-anticlines developed in vertisol at Rayka (Mahi basin) due to the intersection of oppositely directed curvi-planes. Scale is 0.5 m.

Plate 5.3: Close-up view of pedogenic slickensides formed along the surface of a parallelepiped in a vertisol. Location = Mahudi, Sabarmati basin. Diameter of coin is 2.8 cm.

Plate 5.4: Vertisol at Rayka, Mahi basin, showing development of peds, carbonate impregnated fissures and large calcrete nodules disseminated throughout the profile. Length of marker is 8 cm.

Plate 5.5: Red-bed at Dabka (Mahi basin) seen nearly bisecting the section. Thickness of red-bed is 3.5 m.

Plate 5.6: Red-bed of pedogenic origin at Hirpura (Sabarmati basin). Note the loss in reddening towards the base which is associated with a concomitant loss in clay content also. Length of hammer is 32 cm.

Plate 5.7: Cross-stratification within the red-bed suggesting the derived nature of the rubified sediment. Lenght of hammer is 32 cm. Location = Waghpur, Sabarmati basin.

Plate 5.8: Section of vertisol nodules showing a 'ped' nucleus of varying dimensions with respect to the outer carbonate shell. Diameter of coin is 2.5 cm.

Plate 5.9: Decimetre size disorthic calcrete nodules in the vertisol at Rayka, Mahi basin. Diameter of the lens cap is 5.5 cm.

Plate 5.10: Disorthic calcrete nodules associated with a pedogenic red-bed forming a broad band about 0.5 m thick. Scale is 0.5 m. Location = Dabka, Mahi basin.

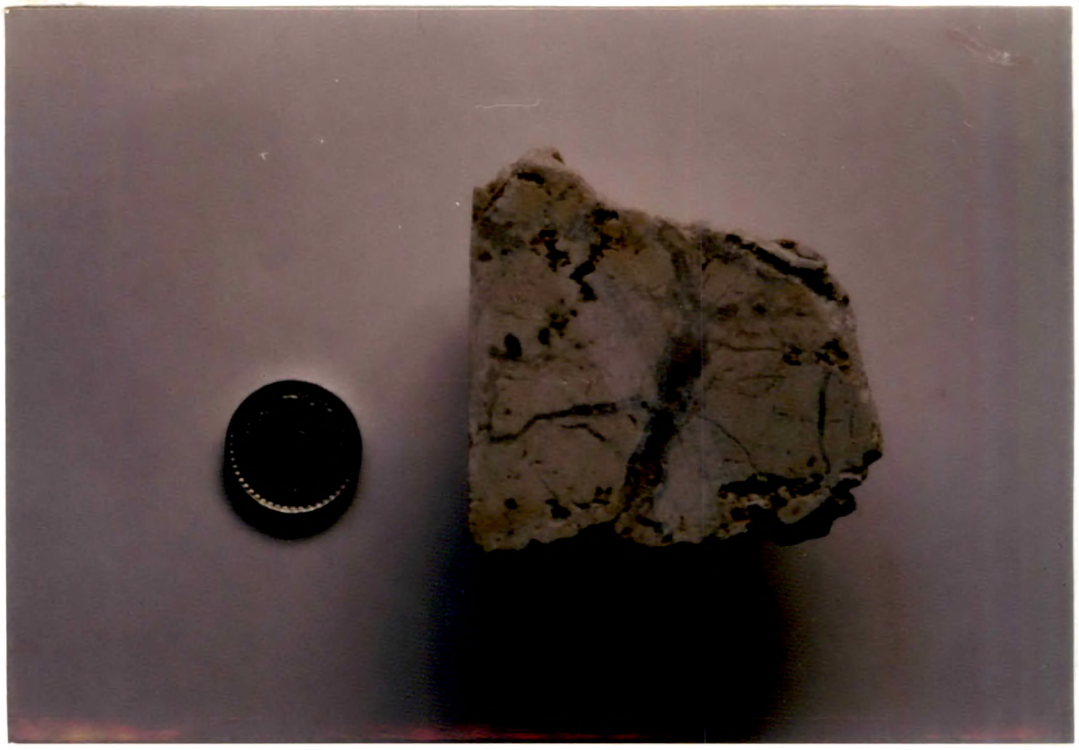

Plate 5.11: Polished section of vertic calcrete nodule from the basal vertisol at Mahudi, Sabramati basin. Note the intense network of spar filled veins seen traversing the nodule. Diameter of coin is 2.5 cm.

Plate 5.12: Groundwater calcrete sheets seen following stratification planes of a channel-fill sand body at Rayka, Mahi basin. Height of figure is 1.55 cm.

Plate 5.13: Discontinuous groundwater calcretes seen developed along stratification planes within Sh facies. Diameter of lens cap is 5.5 cm. (Location = Rayka, Mahi basin).

Plate 5.14: Field photograph of cauliflower calcretes. Note the density of calcretes within the host sediment and the size. Length of the hammer is 32 cm.

Plate 5.15: Polished section of a cauliflower calcrete showing clay and spar filled shrinkage planes traversing the micritic nodule. Diameter of coin is 2·5 cm. (Location = Mahudi, Sabarmati basin).

Plate 5.16: Rhizoliths from vertic soils from Rayka, Mahi basin. Scale is in centimetres.

Plate 5.17: Rhizogenic calcretes from pedogenic red-bed at Dabka, Mahi basin. Note that in comparison to the rhizoliths from vertic soils these are smaller in dimensions and are 'agglutinated'. Scale is in centimetres.

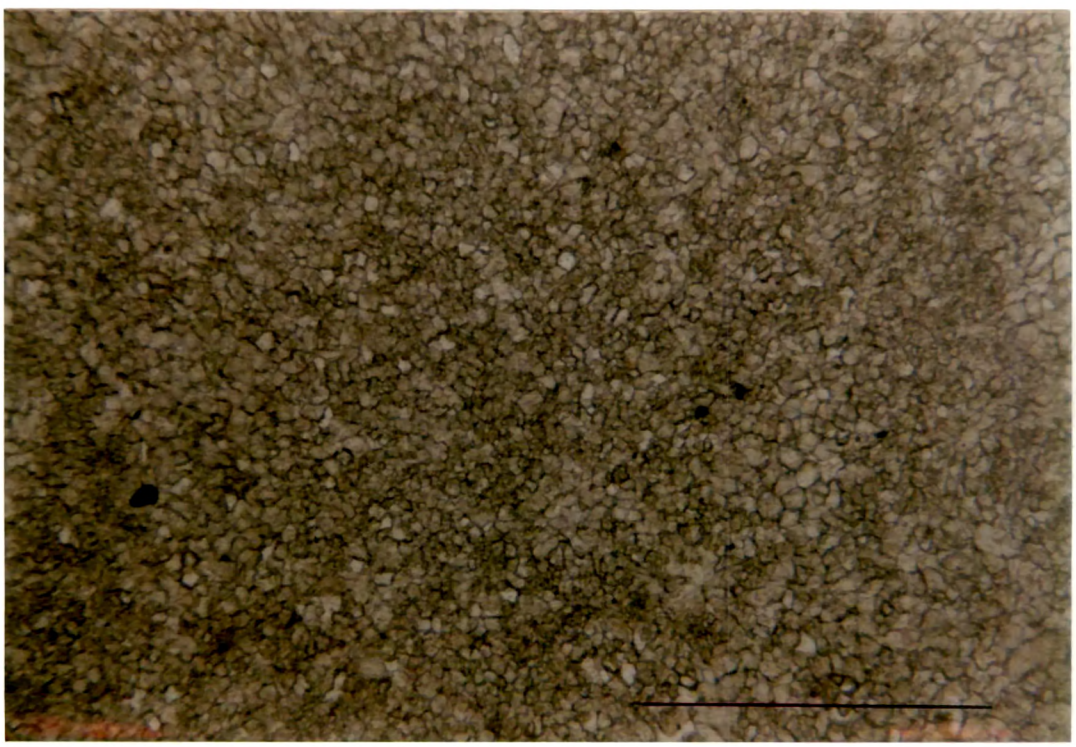

Plate 5.18: Photomicrograph of clotted micrite. Sample is of a vertic pedogenic calcrete (Mahudi, Sabarmati basin). Bar = 50 μm.

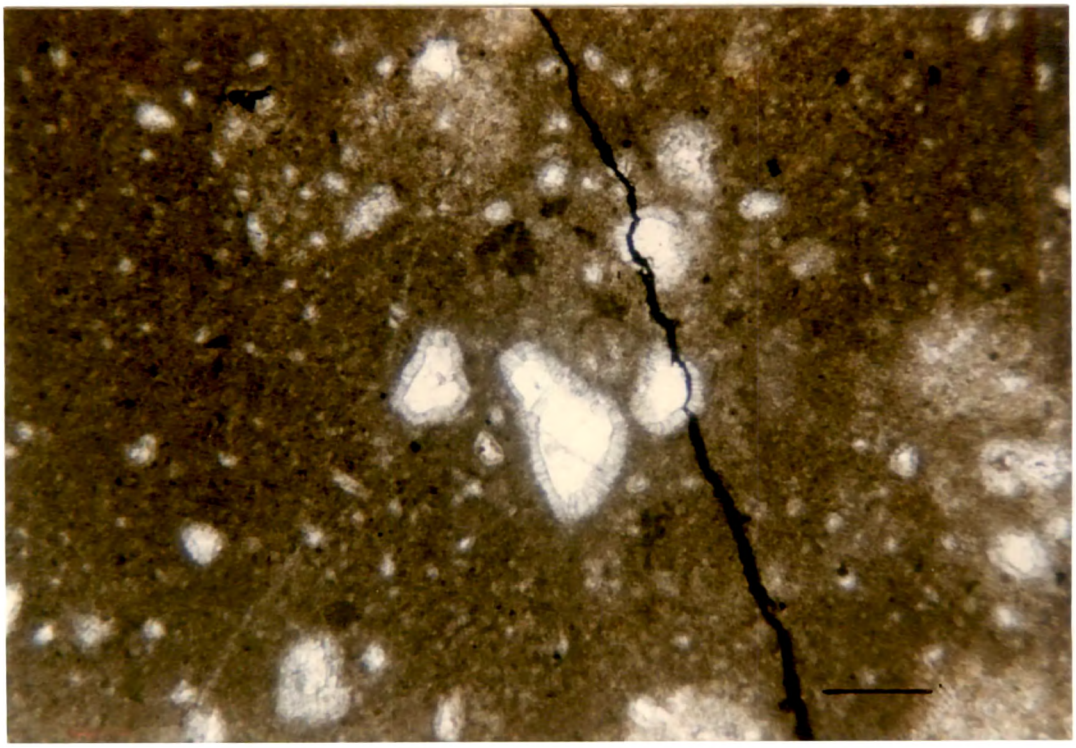

Plate 5.19: Photomicrograph of radial grain coat of needle calcite on quartz clasts floating in a micritic groundmass. Sample is of cauliflower calcrete from Mahudi, Sabarmati basin. Bar = 50 μm.

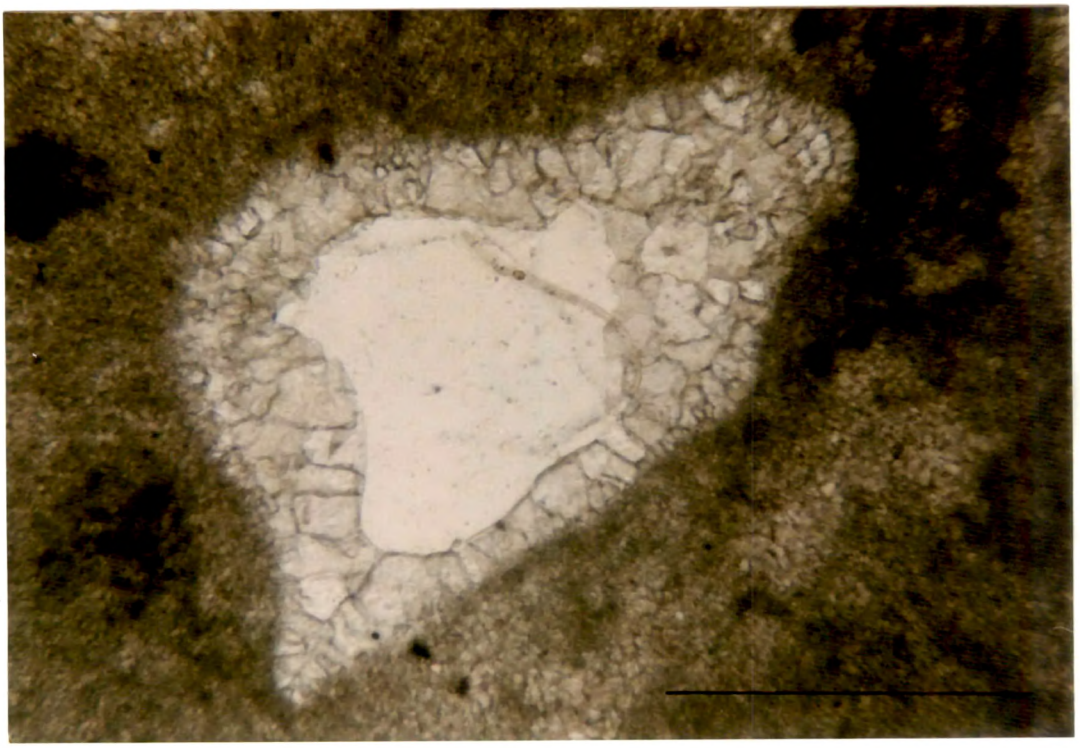

Plate 5.20: Sparitic growth from the pore-wall towards the quartz grain mimicking grain coat fabrics. Note the increase in calcite crystal size towards the grain. Sample is of cauliflower calcrete, Mahudi, Sabarmati basin. Bar = 50 μm.

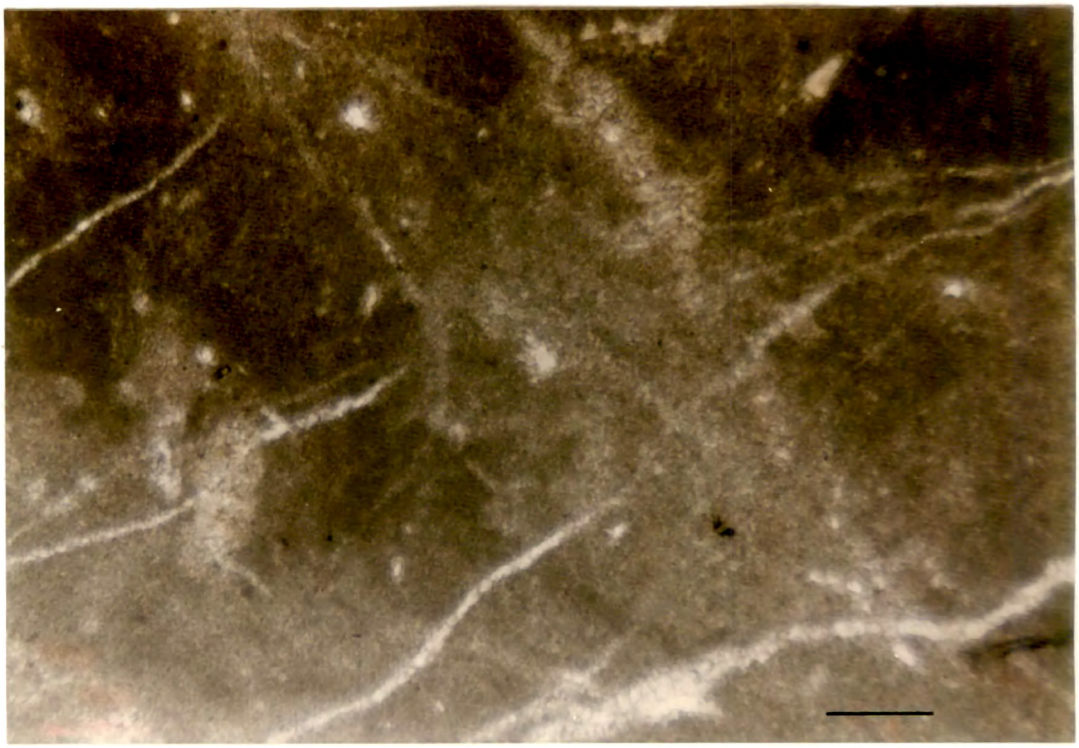

Plate 5.21: Photomicrograph of calcite veins traversing the micritic groundmass. These veins might probably be relicts of root channels that were later infilled by micrspar. Bar = 50 μm. Sample is of vertic calcrete, Mahudi, Sabarmati basin.

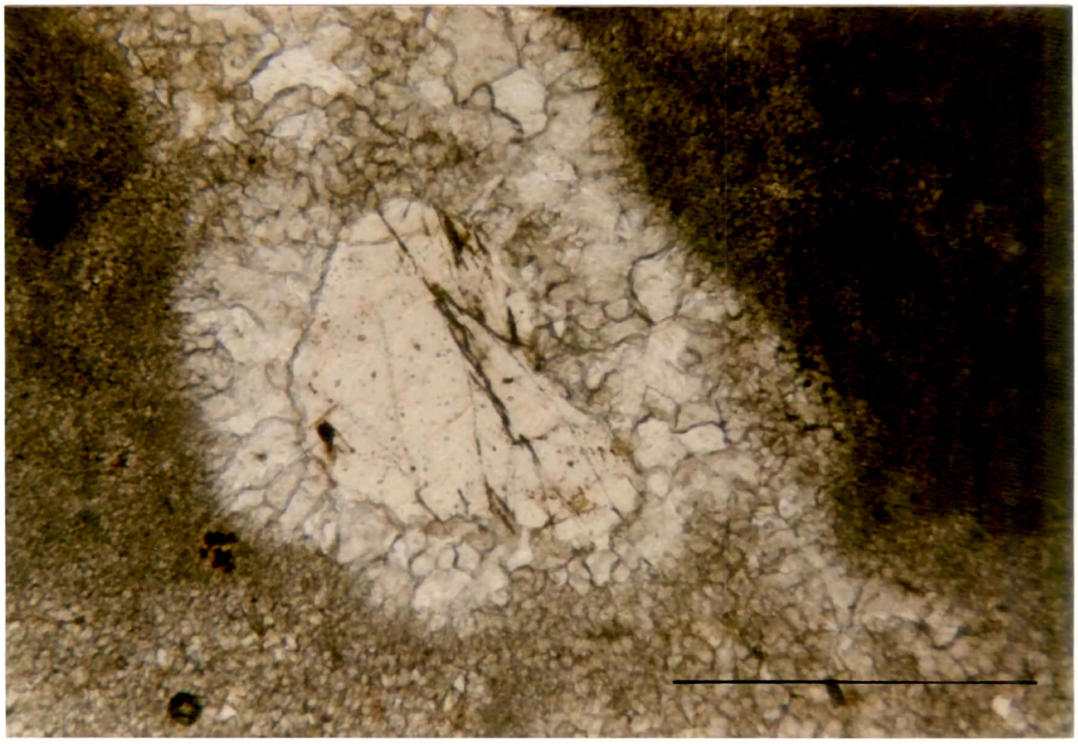

Plate 5.22: Corroded margin of quartz clast due to initial dissolution during the interaction of meteoric waters with the grain. Note the outwardly directed 'c' shaped pits. Bar = 50 μm. Sample is of cauliflower calcrete, Mahudi, Sabarmati basin.

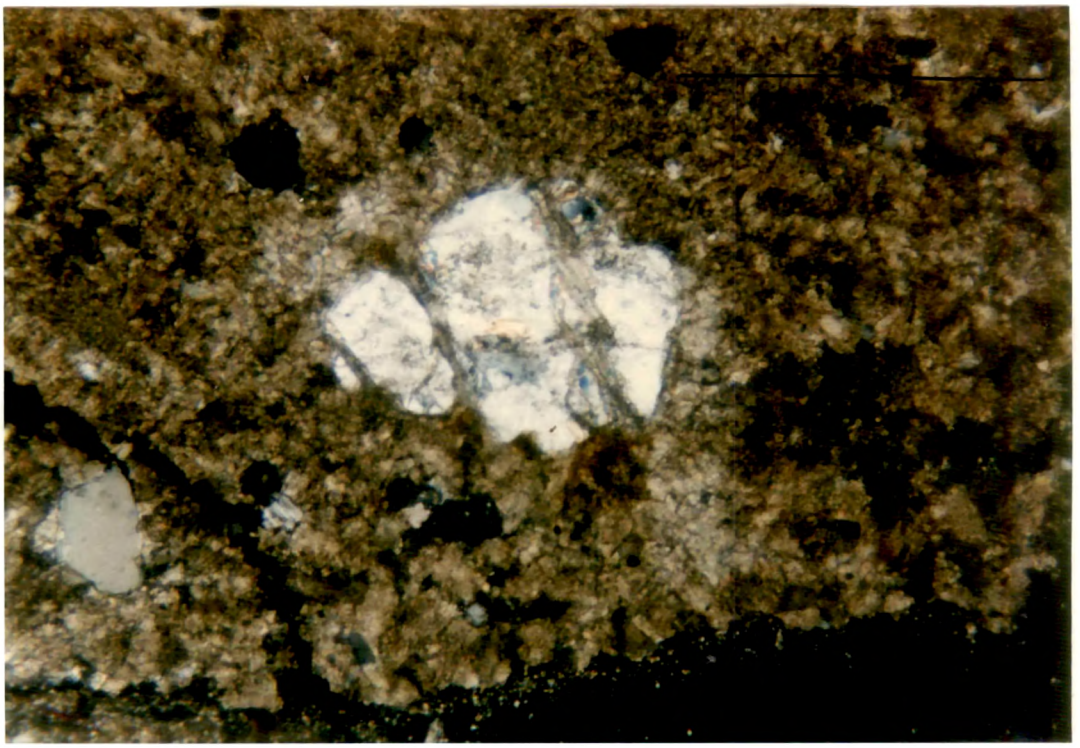

Plate 5.23: Exploding microcline grain due to the displacive growth of calcite. Crossed nicols, bar = 50 μm. Sample is of cauliflower calcrete, Mahudi, Sabarmati basin.

Plate 5.24: Pedogenesis of groundwater calcretes showing relicts preserved within a soil profile, before complete redistribution of the carbonate. Length of hammer is 28 cm. Location = Rayka, Mahi basin.

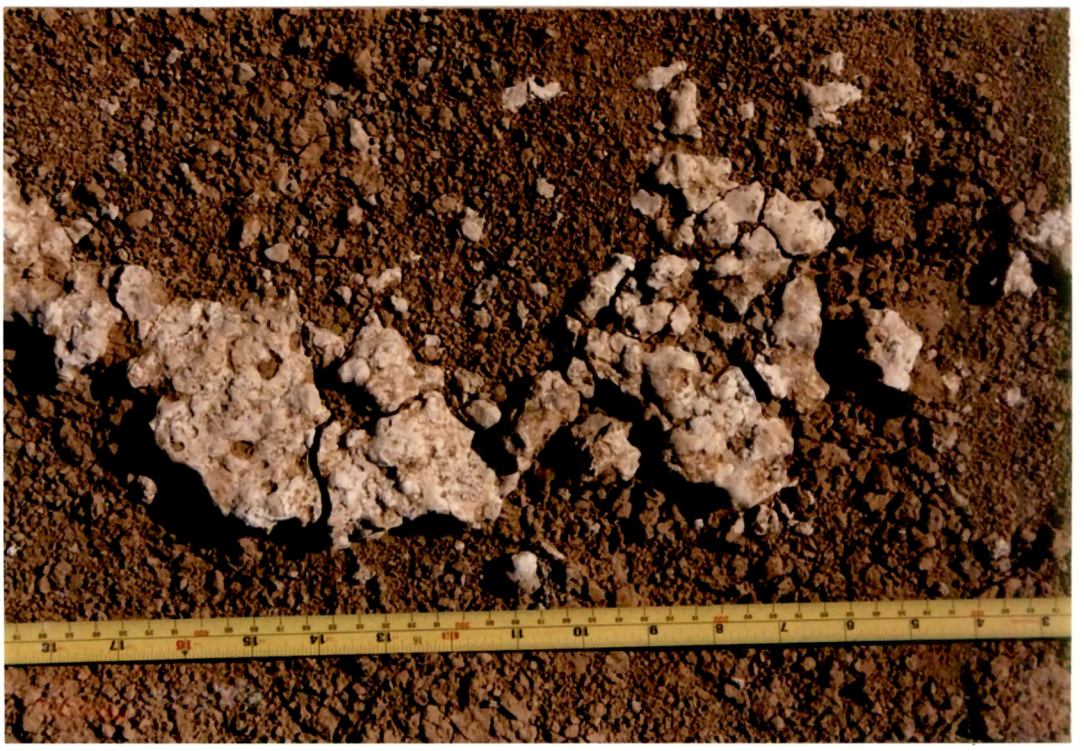

Plate 5.25: Close-up of disruption of groundwater calcrete sheets during pedogenesis leading to the development of smaller nodules. Upper part of the scale is in millimetres. Location = Rayka, Mahi basin.